

# 第25回 N M R 討 論 会

## 講演要旨集

共催 日本化学会・日本生化学会・日本生物物理学会  
日本薬学会・日本農芸化学会・日本分析化学会

日時 昭和61年11月12日(水)～14日(金)

会場 農協ホール (東京都千代田区)



## 第25回NMR討論会

共催 日本化学会・日本生化学会・日本生物物理学会  
日本薬学会・日本農芸化学会・日本分析化学会

日時 昭和61年11月12日(水)～14日(金)

会場 農協ホール(東京都千代田区大手町 1-8-3)  
討論を含めA講演(\*印)20分, B講演 13分  
招待講演(L) 45分, 英語講演(E) 15分

### プログラム

11月12日(水)

12:30-13:22 座長: 京極 好正

1. NMRによるヒト脳腫瘍髄腔内播種の診断について  
(熊本大医化学・脳神経外科) 山崎 政城・吉岡 進
2. 骨組織の T<sub>1</sub> 緩和時間に関する研究  
(京都第一赤十字病院・京都府医大・生理研) 野口 昌彦・日下 義章・三船 哲郎・日下部 虎夫・山下 文治・榊田 喜三郎・西川 弘恭・瀬尾 芳輝
3. <sup>23</sup>Na-, <sup>39</sup>K-NMRによるラット唾液腺細胞内イオン動態の解析  
(生理研・京都府医大) 瀬尾 芳輝・村上 政隆・西川 弘恭・亘 弘
4. 胆汁酸による赤血球膜障害の <sup>31</sup>P-NMR法を用いた検討  
(京都府医大) 中嶋 俊彰・西川 弘恭・瀬戸 良文・中島 年和・島 俊英・奥野 忠雄・瀧野辰郎

13:22-13:55 座長: 金沢 洋子

- 5\* <sup>31</sup>P-飽和移動NMR法による筋細胞内エネルギー輸送の研究  
(京都府医大) 吉崎 和男
6. 光照射下におけるクロレラ細胞の <sup>31</sup>P-NMR saturation transfer  
(国立公害研) 三森 文行

13:55-14:41 座長: 亘 弘

7. リジン発酵菌コリネバクテリウムの <sup>31</sup>P NMRによるポリリン酸の研究  
(東レリサーチセ・東レ基礎研) 川口 謙・丸山 花子・松本 俊一
8. <sup>19</sup>F NMRによるフッ素標識単糖類の生体内動態の研究  
(九大薬) 桃園 裕子・金沢 洋子・原田平 輝志・前田 稔・小嶋 正治

- 9\* 回転する磁場勾配を用いたNMRイメージング - 信号の特異性  
(日立中研) 松井 茂・河野 秀樹

15:10-15:49 座長: 瀬戸 治男

10.  $^1\text{H}$ -NMRによる糖脂質糖鎖の化学構造の解析  
(都臨床研) 神田 大輔・児玉 千恵・鈴木 明身・稲垣 冬彦
11. 核酸関連化合物の N-15 NMRスペクトル  
(理研) 鶴沢 洵, 安斉 謙太郎
12. CCKオクタペプチドの溶液内構造について  
(奈良女大理・生理研・九大理) 中沢 隆・亘 弘・矢内原 昇・松隈 純滋・  
草田 祐弘・郷 信広

15:49-16:29 座長: 森島 績

- 13\* 毒素ペプチドのNMRと distance geometry  
(阪大蛋白研・九大理) 大久保 忠恭・小林 祐次・京極 好正・郷 信広
- 14\* 蛋白質の構造変化を指標とした血清アルブミン - リガンド相互作用の解明  
(大日本製薬総研) 老田 哲也

16:29-17:15 座長: 阿久津 秀雄

15. タンパク質のプロトン緩和のシミュレーション・プログラム  
(近畿大医・京大理) 柴田 進・赤坂 一之
- 16\* ヘムタンパク質におけるヘムの再配向ならびに交換反応の機構とその圧力依存性  
(京大工) 石森 浩一郎・青木 正博・森島 績
17. 免疫グロブリンの光CIDNP  
(阪大蛋白研・東大薬) 林 文晶・京極 好正・遠藤 聡史・荒田 洋治

17:15-17:54 座長: 齋藤 肇

18. NMR法による上り蚕絹フィブロインの溶液構造の研究  
(農工大工) 朝倉 哲郎・出村 誠・櫻葉 均
19.  $^2\text{D}$  NMRによる蛋白の水和特性  
(北大低温研) 花房 尚史
20. 配向DNA繊維の  $^2\text{H}$  NMR  
(東薬大・NIH) 神藤 平三郎・Y.Hiyama・D.A.Torchia

11月13日(木)

9:00-9:45 座長:寺尾 武彦

L1 Two dimensional and zero field NMR of oriented molecules  
(U. of California) M.Gochin · D.Hugi-Cleary · M.Luzar · K.Schenker · A.Thayer ·  
A.Pines

9:45-10:30 座長:赤坂 一之

L2 Dipolar SASS NMR Spectroscopy: separation of dipolar powder patterns in  
rotating solids  
(京大理) 寺尾 武彦 · 中井 利仁 · 三浦 等 · 雜賀 亜幌

10:30-11:00 座長:中條 利一郎

E1 Frequency switched inversion pulse and its application to broadband  
decoupling

(日本電子) 藤原 敏道 · 永山 国昭

E2 Determination of the  $^{14}\text{N}$  quadrupole coupling tensors in a single crystal of  
L-histidine hydrochloride monohydrate by NMR spectroscopy

(Univ. British Columbia · 京大理) C.A.McDowell · 内藤 昌 · D.L.Sastry ·  
竹腰 清乃理

11:00-11:30 座長:小林 祐次

E3  $^{13}\text{C}$  NMR spectra of liquid crystalline compounds. 1. 4'-Alkoxy-4-biphenyl-  
carbonitriles

(化技研) 早水 紀久子 · 柳沢 勝 · 山本 修

E4  $^{63}\text{Cu}$  MASNMR of mixed crystals of  $\text{CuY}_x\text{Z}_{1-x}$  (Y=Cl or Br; Z=Br or I) and  
 $\text{Cu}_x\text{Ag}_{1-x}\text{I}$

(三菱製紙感材研 · 日本電子) 遠藤 一央 · 山本 京之介 · 岡地 誠 · 出口 健三 ·  
松下 和弘 · 藤戸 輝昭

12:30-13:05 座長:引地 邦男

E5 Nuclear magnetic resonance of B22-26 pentapeptide and the methyl ester of  
B23-25 tripeptide of insulin

(Shanghai Inst. Biochem.) Q.-L.Shi · Y.-M.Feng · Z.-X.Lu

E6 Mechanism of activation of hormone-sensitive GTP-binding regulatory protein  
by  $F^-$  ion

(東大理・都立大理) 東島 勉・甲斐莊 正恒

13:05-13:50 座長：宮澤 辰雄

L3 2D NMR studies of the specificity of dihydrofolate reductase

(Leicester U.) G.C.K.Roberts

13:50-14:40 座長：永山 国昭

E7 A new strategy to determine the solution structure of a protein using

$^{13}C$ -spectroscopy - a protein proteinase inhibitor SSI

(都立大理) 甲斐莊 正恒・長尾 洋昌・広沢 敦彦

E8 Binding modes of inhibitors to RNase T<sub>1</sub> as studied by NMR

(都臨床研・東大理) 稲垣 冬彦・紫田 康行・嶋田 一夫・宮澤 辰雄

E9 Computer simulation of spin diffusion in proteins

(京大理・近畿大医) 赤坂 一之・柴田 進

15:00-15:45 座長：甲斐莊 正恒

L4 Proton nuclear magnetic resonance studies of proteins of immunological  
interest

(東大薬・阪大微研・阪大蛋白研) 伊藤 涉・遠藤 聡史・武藤 裕・西村 実和・  
東 伸昭・荒田 洋治・坂戸 信夫・藤尾 啓・林 文晶・京極 好正

15:45-16:30 座長：荒田 洋治

L5 Protein structure and dynamics by NMR

(U. Pennsylvania) S.J.Opella

16:30-17:00 座長：神藤 平三郎

E10 Time-resolved  $^{31}P$  NMR studies on energy utilization associated with muscle  
contraction

(大分医大) 山田 和広・田之倉 優・河野 義久・北野 敬明

E11 A  $^1H$ - $^{31}P$  cross-polarization study on *in vivo* systems

(横浜国大工・阪大蛋白研・鳥取大工) 阿久津 秀雄・小田原 孝行・月原 富武・  
京極 好正

17:00-17:45 座長：稲垣 冬彦

L6 Spatial localization techniques for in vivo NMR  
(Oxford U.) R.Freeman

18:00-20:00 懇親会 (農協ビル 8階 第1大会議室)

11月14日(金)

9:00-9:39 座長：高橋 憲助

21. 溶液中の立体配座解析における  $^1\text{H}$  Biselective  $T_1$  の利用  
(神戸女薬大・阪大薬) 杉浦 真喜子・蔡 東玲・高尾 梢雄・藤原 英明
22. 緩和時間法によるストレプトマイシンの化学構造と動的性質の研究  
(阪大薬・神戸女薬大) 渡辺 昌幸・高木 達也・藤原 英明・佐々木 喜男・  
杉浦 真喜子
23. Quinidine類の  $^{13}\text{C}$   $T_1$  とその異方性運動の検討  
(神戸女薬大) 蔡 東玲・杉浦 真喜子・高尾 梢雄

9:39-10:18 座長：鶴沢 洵

24.  $^1\text{H}$  NMRにおける核オーバーハウザー効果を利用した局所麻酔薬とフォスファチジルコリンベシクルとの相互作用研究  
(京大薬・京都薬大) 黒田 義弘・藤原 靖弘
25. 天然有機化合物の構造解析における新しいNOE測定法  
(東大応微研・日本電子) 降旗 一夫・瀬戸 治男・大内 宗城
26. 異種核2量子遷移NMRの天然有機化合物の構造解析への応用 -  $^1\text{H}$ 核測定による感度向上法  
(日本電子・東大応微研) 大内 宗城・横山 修明・福島 裕・降旗 一夫・瀬戸 治男

10:18-10:57 座長：早水 紀久子

27. 中国産半枝蓮 Scutellaria rivularis の新ジテルペノイドの構造 -  
2-D INADEQUATE および  $^1\text{H}$ - $^{13}\text{C}$  long-range couplingの応用  
(富山医薬大・北陸大薬) 菊池 徹・門田 重利・坪野 浩二・富森 毅・木津 治久・  
井本 吉隆
28. フェニルホスフィン類のアルカリ金属塩のNMR  
(名工大) 横山 幸弘・高橋 憲助
29. 金属核NMRの化学シフトに及ぼす溶媒効果のオリジン (II)  
(近畿大理工) 宗像 恵・北川 進・佐々木 学

10:57-11:23 座長：下川 繁三

30. ゲージ不変な INDO 法  
(北見工大) 福井 洋之・三浦 宏一・平井 明彦
31. 微小量スピン  $^{17}\text{O}$  のプロトンの回転系スピン格子緩和時間に及ぼす影響：いくつかのサルフェイトの場合  
(広島大総科) 森本 邦彦

12:30-13:22 座長：竹内 敬人

32. トリフェニルホスホニウムシクロペンタジエニリドにおける水素及び水銀付加の NMR による研究  
(芝浦工大) 永田 親清・山田 郁
33. ポリオレフィン類の  $^{13}\text{C}$  NMR 立体規則性ピークの化学シフトの理論的計算に基づく帰属  
(農工大工) 朝倉 哲郎・西山 祐幸
34. ピリジン N-オキシド類の置換基効果： $^{17}\text{O}$ -および  $^{15}\text{N}$ -NMR 置換基ケミカルシフト  
(阪大産研) 沢田 正実・高井 嘉雄・木村 聡・山野 智・三角 荘一・都野 雄甫・花房 昭静
35. 阪大産研材料解析総合システム (TASMAC) における NMR の機能  
(阪大産研) 高井 嘉雄・山田 等・福田 房子・田中 高紀・沢田 正実・花房 昭静

13:22-14:08 座長：藤原 英明

36. NMR による高分子膜中の低分子の挙動 (III) - 三酢酸セルロース膜とセルロース膜の比較  
(化技研) 松村 和紀・早水 紀久子・中根 堯・柳下 宏・山本 修
37. 芳香族ポリアミドイミドおよび関連化合物の構造解析における NOE の利用  
(東レリサーチセ) 横田 克行
- 38\* 多量子 2 次元 NMR - 高分子の構造解析への応用  
(北大理・日本電子) 伊倉 光彦・安田 学・加藤 徹・引地 邦男・大内 宗城・江口 恵二

14:08-14:41 座長：中川 直哉

39.  $^{19}\text{F}$ ,  $^1\text{H}$  気相高分解能 NMR による 1,2-ジフルオロエタンの配座エネルギーの測定  
(東大工) 野々山 信二・宮島 隆・川村 時治・平野 恒夫
- 40\* 差分 NMR 法、左右大脳半球機能差の計測  
(電総研) 亀井 裕孟・片山 義朗・横山 浩



15:00-15:52 座長：安藤 勲

41. 結晶中ピリジニウムイオンの運動と  $^1\text{H}$  NMR  
(名大理) 伊藤 ゆかり・浅地 哲夫・池田 龍一・中村 大雄
42. 二三の固体試料中の  $^{13}\text{C}$  スピン交換に関する二次元NMR  
(京大化研) 陳 宜宜, 堀井 文敬・北丸 竜三
43. 高分子多相系の  $^1\text{H}$  スピン拡散に関するCP  $^{13}\text{C}$  NMR  
(京大化研) 中川 将・堀井 文敬・北丸 竜三
44. 固体高分解能NMRによるプラズマ重合膜の解析  
(豊田中研) 田嶋 一郎・山本 豊

15:52-16:44 座長：横山 茂之

45.  $^{13}\text{C}$  VT-MAS NMRによる固体高分子の構造の研究  
(日本電子・東工大) 藤戸 輝昭・出口 健三・今成 司・安藤 勲・山延 健
46. 固体ポリアセチレンの  $^{13}\text{C}$  NMR化学シフトと電子構造  
(東工大) 山延 健・安藤 勲
47. 固体状態におけるグリシン残基の  $^{13}\text{C}$  化学シフトと水素結合の相関  
(東工大・群大工短大・クラレ中研) 安藤 慎治・山延 健・安藤 勲・荘司 顕・  
尾崎 拓男・網屋 繁俊
48.  $^{15}\text{N}$  CP-MAS NMR [III],  $^{15}\text{N}$  標識L-アラニン残基を含む種々のコポリ  
ペプチドの固体構造と $^{15}\text{N}$ 化学シフトとの関係  
(群大工短大・日本電子・東工大) 荘司 顕・尾崎 拓男・藤戸 輝昭・出口 健三・  
安藤 慎二・安藤 勲

16:44-17:30 座長：山本 修

49. ポリ( $\beta$ -ベンジル-L-アスパルテート)鎖中に巻き込ませたL-アラニン残基のコン  
ホメーションと固体  $^{13}\text{C}$  NMR化学シフト  
(東工大・国立がんセ研・群大工短大) 辻 暁・甲本 忠史・安藤 勲・齋藤 肇・  
荘司 顕・尾崎 拓男
50.  $^{23}\text{Na}$  高分解能NMR. ナトリウムコンプレックスの固体および溶液構造の直接比較  
(国立がんセ研) 齋藤 肇・多部田 涼子
- 51\*  $^{13}\text{C}$  固体高分解能NMR: イオノフォア抗生物質の金属イオン結合による構造変化の  
検出(国立がんセ研) 齋藤 肇・多部田 涼子



**THE 25TH NMR SYMPOSIUM (JAPAN)**

**Noukyou Hall, Tokyo**

**November 12-14, 1986**

**The Chemical Society of Japan**

**The Japanese Biochemical Society**

**The Biophysical Society of Japan**

**The Pharmaceutical Society of Japan**

**The Agricultural Chemical Society of Japan**

**The Japan Society for Analytical Chemistry**

## PROGRAM

Wednesday, November 12, 1986

### CONTRIBUTED PAPERS

12:30-13:22 Chairman: Y. Kyogoku

1. NMR Study of Human Cerebrospinal Fluid in The Diagnosis of Subarachnoid Dissemination of Brain Tumors  
**M. Yamasaki** and S. Yoshioka
2. Study on  $^1\text{H}$ -NMR Relaxation Time ( $T_1$ ) of Rabbit Bone  
**M. Noguchi**, Y. Kusaka, T. Mifune, T. Kusakabe, F. Yamashita, K. Sakakida, H. Nishikawa and Y. Seo
3. Measurement of Intracellular  $^{23}\text{Na}$  and  $^{39}\text{K}$  in Perfused Rat Salivary Gland by NMR Spectroscopy  
Y. Seo, M. Murakami, H. Nishikawa and H. Watari
4. Bile Acid-Induced Erythrocyte Membrane Damage Studied by  $^{31}\text{P}$ -NMR  
T. Nakashima, H. Nishikawa, Y. Seto, T. Nakajima, T. Shima, T. Okuno and T. Takino

13:22-13:55 Chairwoman: Y. Kanazawa

5. Intracellular Energy Transport in Muscle Studied by NMR  
**K. Yoshizaki**
6. The Flux of Pi to ATP in *Chlorella vulgaris* Cells under Illumination Measured by P-31 NMR Saturation Transfer  
**F. Mitsumori**

13:55-14:41 Chaiman: H. Watari

7. Polyphosphate Metabolism in *Corynebacterium glutamicum* as Studied by  $^{31}\text{P}$  Nuclear Magnetic Resonance  
**K. Kawaguchi**, H. Maruyama and S. Matsumoto
8. Metabolic Pathway of Fluorinated Hexoses in Mice: A  $^{19}\text{F}$  NMR Study  
Y. Momozono, Y. Kanazawa, T. Haradahira, M. Maeda and M. Kojima
9. NMR Imaging with A Rotary Field Gradient. The Signal with Unusual Properties  
**S. Matsui** and H. Kohno

15:10-15:49 Chairman: H. Seto

10. Analysis of The Chemical Structure of Sugar Chains of Glycolipids by  $^1\text{H}$  Nuclear Magnetic Resonance  
D. Kohda, C. Kodama, A. Suzuki and F. Inagaki
11. N-15 NMR Spectra of Nucleoside Derivatives  
J. Uzawa and K. Anzai
12. The Solution Conformation of Cholecystokinin Octapeptide  
T. Nakazawa, H. Watari, N. Yanaihara, J. Matsukuma, S. Kusada and N. Go

15:49-16:29 Chairman: I. Morishima

13. Conformational Analysis of Toxin Peptide by  $^1\text{H}$ -NMR and Distance Geometry  
T. Ohkubo, Y. Kobayashi, Y. Kyogoku and N. Go
14. Classification of Interactions of Human Serum Albumin with Ligand Molecules as Studied by Proton NMR Spectroscopy  
T. Oida

16:29-17:15 Chairman: H. Akutsu

15. Computer Simulation Program for Proton Relaxation in Proteins  
S. Shibata and K. Akasaka
16. The Mechanism and The Pressure Dependence of Heme Re-orientation and Heme Exchange Reaction of Hemoproteins  
K. Ishimori, M. Aoki and I. Morishima
17. Photo CIDNP Studies of Immunoglobulins  
F. Hayashi, Y. Kyogoku, S. Endo and Y. Arata

17:15-17:54 Chairman: H. Saitô

18. NMR Study of *Philosamia cynthia ricini* Silk Fibroin Structure in Solution  
T. Asakura, M. Demura and H. Kashiba
19. Characteristics of Protein Hydration by  $^2\text{H}$  NMR  
N. Hanafusa
20. Deuterium NMR Study of Oriented DNA Fibers  
H. Shindo, Y. Hiyama and D. A. Torchia

Thursday, November 13, 1986

INVITED LECTURES

9:00-9:45 Chairman: T. Terao

- L1 Two Dimensional and Zero Field NMR of Oriented Molecules  
M. Gochin, D. Hugi-Cleary, M. Luzar, K. Schenker,  
A. Thayer and **A. Pines**

9:45-10:30 Chairman: K. Akasaka

- L2 Dipolar SASS NMR Spectroscopy: Separation of Dipolar  
Powder Patterns in Rotating Solids  
**T. Terao**, T. Nakai, H. Miura and A. Saika

CONTRIBUTED PAPERS

10:30-11:00 Chairman: R. Chujo

- E1 Frequency Switched Inversion Pulse and Its Application  
to Broadband Decoupling  
**T. Fujiwara** and K. Nagayama
- E2 Determination of The  $^{14}\text{N}$  Quadrupole Coupling Tensors in A  
Single Crystal of L-Histidine Hydrochloride Monohydrate  
by NMR Spectroscopy  
C. A. McDowell, **A. Naito**, D. L. Sastry and K. Takegoshi

11:00-11:30 Chairman: Y. Kobayashi

- E3  $^{13}\text{C}$  NMR Spectra of Liquid Crystalline Compounds. 1.  
4'-Alkoxy-4-biphenylcarbonitriles  
**K. Hayamizu**, M. Yanagisawa and O. Yamamoto
- E4  $^{63}\text{Cu}$  MAS NMR of Mixed Crystals of  $\text{CuY}_x\text{Z}_{1-x}$  (Y = Cl or Br;  
Z = Br or I) and  $\text{Cu}_x\text{Ag}_{1-x}\text{I}$   
**K. Endo**, K. Yamamoto, M. Okaji, K. Deguchi,  
K. Matsushita and T. Fujito

12:30-13:05 Chairman: K. Hikichi

- E5 Nuclear Magnetic Resonance of B22-26 Pentapeptide and  
The Methyl Ester of B23-25 Tripeptide of Insulin  
**Q.-L. Shi**, Y.-M. Feng and Z.-X. Lu

- E6 Mechanism of Activation of Hormone-Sensitive GTP-Binding  
Regulatory Protein by F<sup>-</sup> Ion  
**T. Higashijima** and **M. Kainosho**

**INVITED LECTURE**

**13:05-13:50** Chairman: **T. Miyazawa**

- L3 2D NMR Studies of The Specificity of Dihydrofolate  
Reductase  
**G. C. K. Roberts**

**CONTRIBUTED PAPERS**

**13:50-14:40** Chairman: **K. Nagayama**

- E7 A New Strategy to Determine The Solution Structure of A  
Protein Using <sup>13</sup>C-Spectroscopy - A Protein Proteinase  
Inhibitor SSI  
**M. Kainosho**, **H. Nagao** and **A. Hirose**
- E8 Binding Modes of Inhibitors and A Substrate Analog to  
Ribonuclease T<sub>1</sub> as Studied by NMR  
**F. Inagaki**, **Y. Shibata**, **I. Shimada** and **T. Miyazawa**
- E9 Computer Simulation of Spin Diffusion in Proteins  
**K. Akasaka** and **S. Shibata**

**INVITED LECTURES**

**15:00-15:45** Chairman: **M. Kainosho**

- L4 Proton Nuclear Magnetic Resonance Studies of Proteins  
of Immunological Interest  
**W. Ito**, **S. Endo**, **Y. Muto**, **M. Nishimura**, **N. Higashi**,  
**Y. Arata**, **N. Sakato**, **H. Fujio**, **F. Hayashi** and  
**Y. Kyogoku**

**15:45-16:30** Chairman: **Y. Arata**

- L5 Protein Structure and Dynamics by NMR  
**S. J. Opella**

**CONTRIBUTED PAPERS**

**16:30-17:00** Chairman: **H. Shindo**

E10 Time-Resolved  $^{31}\text{P}$  NMR Studies on Energy Utilization  
Associated with Muscle Contraction

**K. Yamada**, M. Tanokura, Y. Kawano and T. Kitano

E11 A  $^1\text{H}$ - $^{31}\text{P}$  Cross-Polarization Study on *In Vivo* Systems

**H. Akutsu**, T. Odahara, T. Tsukihara and Y. Kyogoku

#### INVITED LECTURE

17:00-17:45 Chairman: F. Inagaki

L6 Spatial Localization Techniques for *In Vivo* NMR

**R. Freeman**

#### BUFFET PARTY

18:00-20:00 Conference Room (Noukyou Building, 8th Floor)

Friday, November 14, 1986

#### CONTRIBUTED PAPERS

9:00-9:39 Chairman: K. Takahashi

21. Application of  $^1\text{H}$  Biselective  $T_1$  Data on Conformational  
Analyses in Solution

**M. Sugiura**, T. Sai, N. Takao and H. Fujiwara

22. Molecular Dynamics and Chemical Structure of Streptomycin  
in Solution Determined from Relaxation Time Analysis

**M. Watanabe**, H. Fujiwara, T. Takagi, Y. Sasaki and  
M. Sugiura

23.  $^{13}\text{C}$   $T_1$  Studies of The Anisotropic Motion of Quinidine  
Derivatives

**T. Sai**, M. Sugiura and N. Takao

9:39-10:18 Chairman: J. Uzawa

24. Locations of Local Anesthetics and Their Dynamical  
Perturbations for Lipids in Phosphatidylcholine Vesicles  
as Studied by Nuclear Overhauser Effects in  $^1\text{H}$  Nuclear  
Magnetic Resonance Spectroscopy

**Y. Kuroda** and Y. Fujiwara



25. A New NOE Technique Using Highly Selective Irradiation Frequency Useful for Structural Studies of Natural Products

**K. Furihata**, H. Seto and M. Ohuchi

26. Application of Heteronuclear Double Quantum Coherence NMR for Structural Studies of Natural Products

**M. Ohuchi**, N. Yokoyama, Y. Fukushima, K. Furihata and H. Seto

10:18-10:57 Chairwoman: K. Hayamizu

27. Structures of New Triterpenoids from Chinese Crude Drug "Ban Zhi Lian" (*Scutellaria rivularis*) - Application of 2-D INADEQUATE and Long-Range  $^1\text{H}$ - $^{13}\text{C}$  COSY

T. Kikuchi, **S. Kadota**, K. Tsubono, T. Tomimori, H. Kizu and Y. Imoto

28.  $^{13}\text{C}$  and  $^{31}\text{P}$  NMR Study of Organic Anions Produced from Phenyl and Diphenylphosphines

**Y. Yokoyama** and K. Takahashi

29. The Origin of Solvent Effect on The Chemical Shift of Metal Nuclear Magnetic Resonance

**M. Munakata**, S. Kitagawa and M. Sasaki

10:57-11:23 Chairman: S. Shimokawa

30. Calculation of NMR Chemical Shifts by A Gauge-Invariant INDO Method

**H. Fukui**, K. Miura and A. Hirai

31. Effect of Rare Spin  $^{17}\text{O}$  on The Spin-Lattice Relaxation Time  $T_{1\rho}$  of Protons in The Rotating Frame: Study in Some Sulfates

**K. Morimoto**

12:30-13:22 Chairman: Y. Takeuchi

32. Nuclear Magnetic Resonance Studies of Protonation and Mercuriation of Triphenylphosphonium Cyclopentadienilide

**C. Nagata** and K. Yamada

33. Assignment of The  $^{13}\text{C}$  NMR Resonances of Poly(olefins) to The Tacticity on The Basis of The Chemical Shift Calculation

**T. Asakura** and Y. Nishiyama

34.  $^{15}\text{N}$ - and  $^{17}\text{O}$ -NMR Substituent Chemical Shifts of Pyridine 1-Oxides: A Multiple Multinuclear Approach to The Dual Resonance Effects

**M. Sawada**, Y. Takai, S. Kimura, S. Yamano, S. Misumi, Y. Tsuno and T. Hanafusa

35. Functions and Characteristics of The NMR Section in The Supermini-Computer System of Material Analysis Center (TASMAC): FID Data Receive, Processing, and Linkage to Chemics

**Y. Takai**, H. Yamada, F. Fukuda, T. Tanaka, M. Sawada and T. Hanafusa

**13:22-14:08** Chairman: H. Fujiwara

36. NMR Studies of Behavior of Molecules in Polymer Films (III); Comparison between Cellulose-Triacetate and Cellulose Films

**K. Matsumura**, K. Hayamizu, T. Nakane, H. Yanagishita and O. Yamamoto

37. Use of The Nuclear Overhauser Effect for Structure-Analysis Studies of Aromatic Polyamideimides and Related Compounds

**K. Yokota**

38. Multiple Quantum 2D-NMR: Application to Structural Analysis of Polymers

**M. Ikura**, M. Yasuda, T. Katoh, K. Hikichi, M. Ohuchi and K. Eguchi

**14:08-14:41** Chairman: N. Nakagawa

39. Gas-Phase  $^{19}\text{F}$  and  $^1\text{H}$  High-Resolution NMR Spectroscopy: Application to The Study of Unperturbed Conformational Energies of 1,2-Difluoroethane

**S. Nonoyama**, T. Miyajima, T. Kawamura and T. Hirano

40. A Non-Invasive Method to Detect The Difference in Functions of Cerebral Hemispheres by "Differential NMR"

**H. Kamei**, Y. Katayama and H. Yokoyama

**15:00-15:52** Chairman: I. Ando

41. Molecular Dynamics of Pyridinium Ions in Solid as Studied by  $^1\text{H}$  NMR

Y. Ito, T. Asaji, **R. Ikeda** and D. Nakamura

42. Observation of  $^{13}\text{C}$  Spin Exchanges in Solids by Two-Dimensional NMR Spectroscopy  
Y. Y. Chen, **F. Horii** and R. Kitamaru
43. CP/MAS  $^{13}\text{C}$  NMR Study of  $^1\text{H}$  Spin Diffusion in The Polymeric Multi-Phase System  
**M. Nakagawa**, F. Horii and R. Kitamaru
44. Structural Analysis of Plasma Polymerized Film by High-Resolution Solid-State NMR. Polyacrylonitrile  
**I. Tajima**, T. Suda, M. Yamamoto, K. Satta and H. Morimoto
- 15:52-16:44** Chairman: S. Yokoyama
45. Polymer Structure in The Solid State as Studied by  $^{13}\text{C}$  VT-MAS NMR  
T. Fujito, K. Deguchi, M. Imanari, **I. Ando** and T. Yamanobe
46.  $^{13}\text{C}$  NMR chemical Shift and Electronic Structure of Cis and Trans Polyacetylenes in The Solid State  
**T. Yamanobe** and I. Ando
47. Hydrogen Bonding Effect on the  $^{13}\text{C}$  NMR Chemical Shift of Glycine Residue Carbonyl Carbons in Glycine-Containing Peptides in The Solid State  
**S. Ando**, T. Yamanobe, I. Ando, A. Shoji, T. Ozaki and S. Amiya
48.  $^{15}\text{N}$  CP-MAS NMR [III]. A Study on The Relationship between The Solid Conformation and The  $^{15}\text{N}$  Chemical Shift of  $^{15}\text{N}$  Labeled L-Alanine Residues in Various Copolypeptides  
A. Shoji, **T. Ozaki**, T. Fujito, K. Deguchi, S. Ando and I. Ando
- 16:44-17:30** Chairman: O. Yamamoto
49. Conformation and  $^{13}\text{C}$  NMR Chemical Shift of L-Alanine Residues Incorporated into Poly( $\beta$ -Benzyl L-Aspartate) in The Solid State  
**S. Tsuji**, T. Komoto, I. Ando, H. Saito, A. Shoji and T. Ozaki
50. Direct Comparison of Tertiary Structures between The Solid and Solution State as Determined by High-Resolution  $^{23}\text{Na}$  NMR Spectroscopy  
H. Saito and **R. Tabeta**
51. Conformational Change of Ionophore Antibiotics by Metal-Ion Binding as Detected by High-Resolution Solid-State  $^{13}\text{C}$  NMR  
**H. Saito** and R. Tabeta



# 講演要旨



NMR Study of Human Cerebrospinal Fluid in the Diagnosis of Subarachnoid Dissemination of Brain Tumors

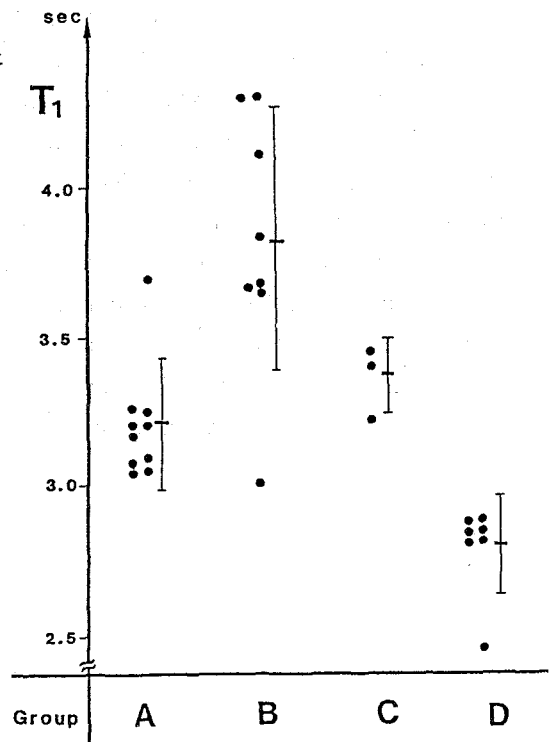
Masaki Yamasaki and \*Susumu Yoshioka

Department of Biochemistry and \*Department of Neurosurgery, Kumamoto University Medical School, Kumamoto

In the diagnosis of brain tumors, it is required to distinguish clearly between the brain tumor with dissemination and the brain tumor without dissemination in the subarachnoid space. The relaxation times ( $T_1$ , proton) of cerebrospinal fluid (CSF) of 28 patients with the brain tumor were studied by nuclear magnetic resonance in order to diagnose definitely CSF dissemination of the brain tumor.

$T_1$  values of the brain tumor with CSF dissemination were shorter than those of the brain tumor without CSF dissemination and did not overlap with the values of the other case as shown in the figure. These data indicate that the brain tumor with CSF dissemination can be clearly distinguished from the brain tumor without dissemination by the use of the relaxation times. Furthermore, these results suggest that  $T_1$  values are useful for the diagnosis of CSF dissemination and malignant glioma.

The relaxation times ( $T_1$ ) of CSF of 28 patients with the brain tumor. Group A; Intramedullary glial tumor. B; Extramedullary tumor. C; Control. D; Brain tumor with CSF dissemination diagnosed by clinical examination, CT-scan, and CSF cytology.



## STUDY ON 1H-NMR RELAXATION TIME(T1) OF RABBIT BONE

M.Noguchi, Y.Kusaka\*, T.Mifune\*, T.Kusakabe\*, F.Yamashita\*, K.Sakakida,\*  
H.Nishikawa\*\*, Y.Seo\*\*\*

Dept. of Orthopaedic Surgery, Kyoto First Red Cross Hospital, Dept. of  
\* Orthopaedic Surgery and Physiology, Kyoto Prefectural University of Medicine,  
\*\*  
\*\*\* National Institute for Physiological Science

Bone is made up of water, lipid, macromolecules that compose the micro-structure, such as collagen, proteoglycan, and hydroxyapatite. The mobilities of water in a bone are determined by its interaction with the macromolecules, and represented by its T1 value. The T1 value of a pathological bone may differ from normal one on account of changes of the micro-structure. In this study, the T1 values and contents of water and lipid were observed by a spin echo NMR technique in normal rabbit bone and fractured one in the process of healing, and then discussed the differences between them. Our findings provide a basis for the possible clinical application of MRI.

Normal cortical and cancellous bones of femurs of male rabbits(0.5-4.0kg) were used as materials. Those bones of fractured fibula of rabbits(2.6-3.5kg) in the process of healing were used as pathological materials. T1 values were measured by spin echo NMR(JNM-FSE-60E) by using IR pulse sequence. Water and lipid contents were measured by both NMR and weight.

The normal cortical bone had a single component of T1 due to water, and normal cancellous bone had two components : the long and short ones due to water and lipid in the bones. T1 due to water in those bones correlated well with each water content. On the other hand, the T1 value of cancellous bone had longer than the one of cortical bone, even if both bones had the same water contents. The short T1(ca.140msec) did not change under any condition.

The T1 value in the process of healing of fractured rabbit fibula decreased gradually as healing.



MEASUREMENT OF INTRACELLULAR  $^{23}\text{Na}$  AND  $^{39}\text{K}$  IN PERFUSED RAT SALIVARY GLAND BY NMR SPECTROSCOPY

Yoshiteru Seo, Masataka Murakami, Hiroyasu Nishikawa, & Hiroshi Watari

Department of Molecular Physiology, National Institute for Physiological Sciences, Okazaki, 444; and Department of Physiology, Kyoto Prefectural University of Medicine, Kyoto, 602, Japan

In the mechanisms of epithelial water and electrolyte transport, Na, K, and Cl play important roles ( $\text{Na}^+/\text{K}^+$  ATPase,  $\text{Na}^+/\text{K}^+/\text{2Cl}^-$  co-transport,  $\text{K}^+$  channel). Especially, the Na gradient across basolateral membrane, which established by  $\text{Na}^+/\text{K}^+$  ATPase, is important as an ionic energy store for epithelial transport. With the onset of secretion by acetylcholine (ACh) in the salivary gland, the increase in K extrusion is well known and considered to support for driving a Na-K-2Cl entry across basolateral membrane. An NMR spectroscopy enabled us to measure the phosphorus energy metabolites of the in vivo organs, non-invasively and continuously. The present study was undertaken using sodium- and potassium- nuclear magnetic resonance ( $^{23}\text{Na}$  and  $^{39}\text{K}$  NMR) to measure intra- and extra-cellular Na and K in the isolated perfused mandibular of rat. The intra- and extra-cellular electrolytes were discriminated by use of the chemical shift reagent,  $\text{Dy}(\text{TTHA})^{3-}$  (dysprosium triethylenetetramine-N,N,N',N'',N''',N''''-hexaacetic acid).  $^{23}\text{Na}$  and  $^{39}\text{K}$  NMR spectra were collected using WM-360wb NMR spectrometer (Bruker) operating at 95.27 and 16.8 MHz, respectively. A broadband tunable probe, 10 mm diameter, was used. The rat submandibular gland (0.2 g wet weight) was isolated and perfused arterially at  $24^\circ\text{C}$ . During control perfusion, the intracellular Na was estimated as around 10 mmol/l ICF. During secretion by 1  $\mu\text{mol/l}$  of acetylcholine (ACh) for 30 min, intracellular Na increased by about 9.1 mmol/l ICF. During perfusion only with ouabain (1 mmol/l),  $\text{Na}_{\text{in}}$  almost unchanged, but the  $\text{Na}_{\text{in}}$  increased drastically by 44 mmol/l ICF during perfusion with ouabain (1 mmol/l) and ACh (1  $\mu\text{mol/l}$ ). Cellular and extracellular K were also discriminated by  $^{39}\text{K}$  NMR spectroscopy. At rest intracellular K was around 135 mmol/l ICF and the level of intracellular K decreased to around 100 mmol/l ICF during the perfusion with ACh (1  $\mu\text{mol/l}$ ) and ouabain (1 mmol/l).

BILE ACID -INDUCED ERYTHROCYTE MEMBRANE DAMAGE STUDIED BY  $^{31}\text{P}$ -NMR  
Toshiaki NAKASHIMA<sup>1)</sup>, Hiroyasu NISHIKAWA<sup>2)</sup>, Yoshifumi SETO<sup>1)</sup>,  
Toshikazu NAKAJIMA<sup>1)</sup>, Toshihide SHIMA<sup>1)</sup>, Tadao OKUNO<sup>1)</sup>,  
Tatsuro TAKINO<sup>1)</sup>

1) Third Department of Internal Medicine, 2) First Department of  
Physiology, Kyoto Prefectural University of Medicine, Kamikyo-ku,  
Kyoto, Japan

To examine the effects of bile acids on biological membrane,  
we analyzed the  $^{31}\text{P}$ -NMR spectra of human erythrocyte ghosts induced  
by various bile acids.

The erythrocyte ghosts prepared according to the method of Dodge  
were further sonicated into small vesicles. The samples were  
incubated with 3-6 mM bile acids at 38 C for 10-30 min in 154 mM  
NaCl (5 mM Tris-HCl buffer, pH 7.4). The  $^{31}\text{P}$ -NMR spectra were  
measured by JEOL-PFT-100 NMR ( $^{31}\text{P}$ : 40.3 MHz, 24,000 Gaus).

As a result, a broad spectrum with two prominent peaks was  
determined in untreated (control) sample; the peak at 10.4 ppm  
originated probably from membrane phospholipid arranged in order  
and that at 0.6 ppm did from disordering phospholipid in the  
menbrane. There were marked differences of  $^{31}\text{P}$ -NMR spectra of  
erythrocyte membrane after each bile acid treatment. These data  
suggest that each bile acid has different effect on biological  
membrane due to it's number of -OH and/or taurine or glycine  
conjugated form.

# INTRACELLULAR ENERGY TRANSPORT IN MUSCLE STUDIED BY NMR.

Kazuo Yoshizaki,

Dept. Physiol., Kyoto Pref. Univ. Med., Kyoto 602,  
Japan

The diffusion rates of ATP and phosphocreatine (PCr), and the flux of creatine kinase (CPK) reaction in muscle were studied to evaluate the energy shuttle hypothesis of PCr and CPK system.

1. Diffusion coefficient of PCr was 1.4 times larger than that of ATP measured by  $^{31}\text{P}$ -pulsed field gradient NMR, suggesting the efficiency of PCr molecule for the intracellular energy transport.

2. The CPK flux ( $770 \text{ nmol}\cdot\text{g}^{-1}\cdot\text{s}^{-1}$ ) in resting smooth muscle of bullfrog stomach obtained by  $^{31}\text{P}$ -saturation transfer NMR was 100 times larger than the ATP turnover rate ( $6.54 \text{ nmol}\cdot\text{g}^{-1}\cdot\text{s}^{-1}$ ) calculated from the oxygen consumption rate with the assumption that  $\text{P/O} = 3$ . Therefore the CPK reaction is at equilibrium in resting smooth muscle of bullfrog stomach.

3. ADP concentration was  $19 \text{ nmol}\cdot\text{g}^{-1}$ , calculated from the CPK equilibrium constant. The life time of ADP molecule was 25 ms using the CPK flux. The mean square length of diffusion (1 dimensional) of ADP molecule was  $3 \mu\text{m}$ , calculated from the diffusion coefficient  $2 \times 10^{-6} \text{ cm}^2 \text{ s}^{-1}$  of ATP. The similar values were obtained using the reported CPK flux on skeletal muscle, heart, and brain.

4. The diffusion length of ADP is larger than the diameter of the myofibril (1~2  $\mu\text{m}$ ). Therefore in heart muscle having the alternate arrangement of mitochondria and myofibril, ADP molecule can move from myofibril to mitochondria without CPK reaction. The energy shuttle hypothesis might be discarded.

THE FLUX OF Pi TO ATP IN CHLORELLA VULGARIS CELLS UNDER  
ILLUMINATION MEASURED BY P-31 NMR SATURATION TRANSFER

Fumiyuki MITSUMORI

National Institute for Environmental Studies, Yatabe, Tsukuba,  
Ibaraki 305, Japan

Chlorella vulgaris 11h, a species of green algae, produces ATP by photophosphorylation in the light as well as glycolysis and oxidative phosphorylation. It has already been shown that the stromal Pi in the chloroplast and the cytoplasmic Pi were separately observed when the suspension of Chlorella cells was illuminated in situ[1,2]. In the present study  $^{31}\text{P}$ -NMR saturation transfer techniques were applied to measure the unidirectional flux of Pi to ATP in Chlorella cells in the light. The flux in the intact multicompartement cell can currently only be measured by NMR. When ATP  $\gamma$  resonance was selectively saturated, 10% and 3% reductions were observed at stromal Pi and cytoplasmic Pi, respectively under illumination. Using the  $T_1$  value of 1.0 s for Pi the fluxes of Pi to ATP were calculated as  $750 \pm 150$  and  $300 \pm 80$   $\text{nmol s}^{-1}(\text{ml packed cell})^{-1}$  at stroma and cytoplasm, respectively. This saturation transfer disappeared in the dark, or in the presence of DCMU, an inhibitor of photosystem II, even in the light. On the other hand,  $\text{O}_2$  evolution rate in the dilute cell suspension was  $201.4 \pm 17.3$   $\text{nmol s}^{-1}(\text{ml packed cell})^{-1}$  in the light. Assuming that the  $\text{H}^+/\text{ATP}$  ratio is 2 at the ATP synthase in the thylakoid membrane, the net photophosphorylation rate was calculated to be  $806 \pm 69$   $\text{nmol s}^{-1}(\text{ml packed cell})^{-1}$ . This value could account for the flux of Pi to ATP observed at stroma by the saturation transfer method.

References:

- [1] F.Mitsumori and O.Ito, FEBS Letters 174, 248-252 (1984)
- [2] F.Mitsumori and O.Ito, J.Magn.Reson. 60, 106-108 (1984)

POLYPHOSPHATE METABOLISM IN CORYNEBACTERIUM GLUTAMICUM AS  
STUDIED BY  $^{31}\text{P}$  NUCLEAR MAGNETIC RESONANCE

Ken Kawaguchi\*, Hanako Maruyama\* and Shunichi Matsumoto\*\*

\* Analytical Sciences Department, Toray Research Center,  
Inc., Kamakura, Kanagawa, Japan

\*\*Basic Research Laboratories, Toray Industries, Inc., Nagoya,  
Aichi, Japan

In vivo  $^{31}\text{P}$  NMR has been used to study the metabolism of polyphosphate in Corynebacterium glutamicum ATCC13286, a bacterium which excretes large quantity of L-lysine into the medium. We observed a remarked resonance of polyphosphate under anaerobic conditions when C. glutamicum ATCC13286 was cultured aerobically to stationary phase in nutrient broth, washed twice with chilled distilled water and resuspended in the water (containing 20%  $\text{D}_2\text{O}$ ), but the resonance was not so remarkable when washed with phosphate buffer (pH 7.6) and resuspended in the same buffer. Upon addition of glucose to the cells resuspended in water, the intensity of the polyphosphate peak decreased dramatically. This is probably due to the reaction catalyzed by polyphosphate glucokinase, in which the phosphate is transferred from polyphosphate to glucose. The enzyme is known to be present in many corynebacteria, but not in E. coli. The decreased intensity of polyphosphate peak by the addition of glucose was recovered in part by air bubbling. The accumulation of polyphosphate under aerobic condition is mediated by polyphosphate kinase, in which the terminal phosphoryl group of ATP is transferred to polyphosphate.

There is little doubt that accumulation of polyphosphate is catalyzed by polyphosphate kinase. On the other hand, the degradative pathway remains still ambiguous. Our results indicate that polyphosphate seems to be utilized for the phosphorylation of hexoses in corynebacteria.

## METABOLIC PATHWAY OF FLUORINATED HEXOSES IN MICE: A $^{19}\text{F}$ NMR STUDY

Yuko Momozono, Yoko Kanazawa, Terushi Haradahira, Minoru Maeda,  
and Masaharu Kojima  
Faculty of Pharmaceutical Sciences, Kyushu University 62,  
Higashi-ku, Maidashi, Fukuoka 812

2-Deoxy-2-fluoro-D-glucose (FDG) has been used for in vivo studies of regional glucose utilization in man by positron emission tomography in the form of  $^{18}\text{F}$  FDG. In this work, in vivo biochemistry and dynamics of FDG in mice was studied by  $^{19}\text{F}$  NMR. The reliability of  $^{19}\text{F}$  NMR method in quantification of fluorinated hexoses and their metabolites in vivo was examined. The present system is extremely suitable for the latter purpose because the dynamics of FDG in the form of total fluorine compounds has been extensively studied by the use of radiolabeled compound  $^{18}\text{F}$  FDG.

Male mice (ddY) were injected intravenously with FDG and 2-deoxy-2-fluoro-D-mannose (FDM) (0.03 - 0.4 mg/g) dissolved in isotonic saline. The excised organs and urine were subjected to NMR measurements with JEOL FX-100 (94 MHz) at ambient temp. ( $25 \pm 1^\circ\text{C}$ ).

FDG and FDM could be distinguished clearly by their chemical shifts. The shift between FDG and its metabolite FDG-6-P or FDM and FDM-6-P was too small for their distinction in tissues. The signals of fluorinated compounds in tissues showed the chemical shift corresponding to the one in hydrophilic media. F signals were found in brain and in heart mostly as mixtures of FDG(-6-P) and FDM(-6-P). Especially in heart where the clearance was slow, a marked interconversion between FDG and FDM was observed. The presence of such reaction could be shown for the first time by this NMR study. This unexpected conversion was demonstrated in vitro by the treatment of the former with phosphoglucose isomerase. The concentrations of total fluorine compounds in organs under various animal conditions determined by  $^{19}\text{F}$  NMR spectra were in good agreement with the  $^{18}\text{F}$  data.

NMR IMAGING WITH A ROTARY FIELD GRADIENT.

THE SIGNAL WITH UNUSUAL PROPERTIES

Shigeru Matsui and Hideki Kohno

Central Research Laboratory, Hitachi, Ltd.

P.O. Box 2, Kokubunji, Tokyo 185, Japan

A new method of imaging has been developed in which signal measurements are taken during rotation of a field gradient. Preliminary experimental results will be reported together with unusual aspects of the present method.

Generally, the phase of the signal measured during the rotation traces a circle in the so-called  $k$  space (Fourier space). This signal provides no useful data that can undergo systematic data processing to yield a spin image, because the circle is not symmetric about the origin of the  $k$  space. The circle, however, can be made symmetric about the origin by prior application of a stationary field gradient. Thus, the resultant signal directly provides symmetric circular phase information. Taking measurements after changing the gradient amplitude (or the rotation frequency) permits a concentric set of circular signals to be obtained. The signal set can be converted to a spin image by suitable data processing involving Fourier transformations along the radii and back projections.

In the present method, the number of projection data is determined by the number of signal sampling points. The image matrix depends on the number of measurements. These aspects are in contrast to the usual projection reconstruction method. Furthermore, for each FID obtained along the radius, the phase development is determined by the gradient effect only, provided that the gradient amplitude is varied as a measurement parameter while the rotation frequency is fixed. As a result, it is possible to obtain an FID shape which is unaffected by field inhomogeneity and transverse relaxation. In addition, an analysis shows that the circular signal can be regarded as a superposition of frequency components over an infinitely wide frequency range. Their frequencies consist of integer multiples of the rotation frequency. Their amplitudes depend on the Bessel functions of the first kind and the spin distribution. This fact imposes two conditions on signal detection, which will be discussed in detail.

ANALYSIS OF THE CHEMICAL STRUCTURE OF SUGAR CHAINS OF  
GLYCOLIPIDS BY  $^1\text{H}$  NUCLEAR MAGNETIC RESONANCE

Daisuke Kohda, Chie Kodama, Akemi Suzuki<sup>†</sup> and Fuyuhiko Inagaki  
Department of Medical Chemistry, <sup>†</sup>Metabolism Section,  
The Tokyo Metropolitan Institute of Medical Science,  
Bunkyo-ku, Tokyo, Japan

Glycolipids are components of cell membranes and are thought to play important roles in higher-order cell functions, such as cell-cell recognition. Clinically, glycolipids are useful as specific markers of tumor cells for diagnosis and therapy of cancers. We need an efficient and nondestructive method for determining the chemical structure of glycolipids. NMR is suitable for this purpose, but the overlaps of sugar proton signals have prevented us from analyzing the spectrum of glycolipids in detail.

In the present study, we applied Multiple-Relayed COSY and NOE techniques of NMR for the determination of the chemical structure of Globoside (GalNAc $\beta$ 1-3Gal $\alpha$ 1-4Gal $\beta$ 1-4Glc $\beta$ 1-Cer in DMSO- $d_6$ ). Using Multiple-Relayed COSY, the magnetization of the anomeric proton is transferred sequentially to the neighbouring protons via spin-spin couplings. Sub-spectrum of each sugar residue can be obtained as a cross section of 2D Multiple-Relayed COSY spectrum of Globoside. From the spin coupling pattern of the extracted sub-spectra of the sugar residues, the types of the sugars can be identified. NOE is subsequently measured to determine the linkage of the sugar chains. Upon selective irradiation of the anomeric proton signal, NOE is observed at the proton signal of the neighbouring residue in addition to the proton signals of the same residue. The linkage of the sugar residues of glycolipids can be determined using the NOE data combined with the assignment of the proton signals made by the Relayed COSY experiment.

We concluded that the chemical structure of sugar moiety of glycolipids can be determined, in principle, nonempirically and nondestructively using NMR information described above. Now we are testing a micro-NMR tube to reduce the sample volume. We expect that the minimal amount of glycolipid is decreased to about 200 $\mu\text{g}$ , which is reasonable amount from practical viewpoint.



## N-15 NMR SPECTRA OF NUCLEOSIDE DERIVATIVES

Jun Uzawa and Kentaro Anzai

The Institute of Physical and Chemical Research, Wako-shi,  
Saitama 351, Japan

The Usefulness of LSPD on C-13 NMR spectra in the structural determination of nucleosides has been shown by the present authors (1-3). This announcement is concerned with our preliminary study on how the structural modifications of adenosine are reflected on N-15 NMR spectra (4).

Introduction of a methyl group at C6-N of adenosine ( $\delta_N$  62.5) caused small upfield shifts of C6-N, N1, and N3 signals. In the case of the compounds where acyl or trityl groups are introduced at C6-N, downfield shifts at C6-N, N1, and N3 were observed: e.g. N<sup>6</sup>, N<sup>6</sup>-di-p-toluyladenine, N1 ( $\Delta$  35 ppm), N3 ( $\Delta$  28 ppm).

Introduction of methyl group at N1 to give neutral N1-methyladenosine or a N1-charged immonium compound resulted in upfield shifts at N1 ( $\Delta$  82 ppm). A similar upfield shift was observed in a N1-methoxy derivative of adenosine ( $\Delta$  24 ppm). Though adenosine and adenosine N1-oxide were indistinguishable in N-15 chemical shifts, a clear difference was observed in  $^2J_{N-1, H-2}$ ; adenosine  $^2J_{N, H} = -13$  Hz; adenosine N-oxide  $^2J_{N, H} = -5$  Hz. The announcement on the decrease of  $^2J_{N, H}$  by quenching the lone pair of nitrogen has a precedent (5). Combing N-15 chemical shifts with  $^2J_{N, H}$ , N-15 NMR spectra seemed to afford useful information about the structure of nucleoside compounds.

- 1) J. Uzawa and M. Uramoto. *Org. Magn. Reson.* 12, 612 (1979).
- 2) J. Uzawa and K. Anzai. *Can. J. Chem.* 62, 1555 (1984).
- 3) J. Uzawa and K. Anzai. *Can. J. Chem.* 63, 3537 (1985).
- 4) No refocussed pulse sequence was used for INEPT. N-15 Chemical shifts were measured relative to (N-15) ammonium nitrate as the external standard.
- 5) R. Wasylshen and T. Schaefer. *Can. J. Chem.* 50, 2989 (1972).

## THE SOLUTION CONFORMATION OF CHOLECYSTOKININ OCTAPEPTIDE

Takashi Nakazawa, Hiroshi Watari\*, Noboru Yanaihara\*  
Junji Matsukuma<sup>#</sup>, Sukehiro Kusada<sup>#</sup> and Nobuhiro Go<sup>#</sup>

Faculty of Science, Nara Women's University, Nara, Japan.

\*Department of Molecular Physiology, National Institute for  
Physiological Science, Okazaki, Aichi, Japan.

<sup>#</sup>Faculty of Science, Kyushu University, Fukuoka, Japan.

Proton nuclear magnetic resonance of cholecystokinin C-terminal octapeptide, Asp<sup>1</sup>-Tyr<sup>2</sup>(SO<sub>3</sub>H)-Met<sup>3</sup>-Gly<sup>4</sup>-Trp<sup>5</sup>-Met<sup>6</sup>-Asp<sup>7</sup>-Phe<sup>8</sup>-NH<sub>2</sub> (CCK-8), in dimethylsulfoxide solution was studied by two dimensional techniques. This peptide stimulates gall bladder contraction and pancreatic juice secretion.

Several structural features of the peptide were elucidated based on the complete assignment of signals and the NOE data obtained from one dimensional NOE-difference spectra and two dimensional NOESY spectra. As well as sequence-specific NOE networks, the NOE between the amide proton of Tyr<sup>2</sup> and the C<sup>α</sup>-proton of Met<sup>6</sup> was observed. These findings suggest that CCK-8 has a looped conformation. The assumption of this looped model for CCK-8 was supported by the measurement of the temperature dependence of amide proton signals, which implied the possibility of intrachain interactions and indicated the presence of a conformational transition at around 320 K. Different from CCK-8, no definite conformations were found for the other peptides, non-sulfated CCK-8 and CCK-7, which have practically no biological activity.

The folding of the main chain was further analyzed by the distance geometry calculations for the hexapeptide moiety of CCK-8 from Asp<sup>1</sup> to Met<sup>6</sup>. The calculations used six NOESY cross peaks by which the upper distance limits were defined, and started from 10 initial structures. As expected from the definition of distance constraints assuming the  $\beta$ -sheet structure, the initial structures converged into looped  $\beta$ -sheet structures being similar to each other. Although no information about the side-chain structure was obtained, the final structure satisfied every distance constraints.

CONFORMATIONAL ANALYSIS OF TOXIN PEPTIDES BY  $^1\text{H}$ -NMR AND  
DISTANCE GEOMETRY

Tadayasu Ohkubo, Yuji Kobayashi, Yoshimasa Kyogoku and  
Nobuhiro Go\*

Institute for Protein Research, Osaka University, Suita,  
Osaka 565 and \*Department of Physics, Faculty of Science,  
Kyushu University, Fukuoka 812, Japan

Recently we have developed a new technique to determine the solution structure of polypeptide with the combined use of  $^1\text{H}$ -NMR and distance geometry algorithm. Two toxin peptides, synthetic analogue of heat-stable enterotoxin ( STh [6-19] ) and conotoxin GI, were investigated by this procedure. STh [6-19] is produced by a human strain of enterotoxigenic Escherichia coli (SK-1) and causes acute diarrhea. Conotoxin GI is a neurotoxic peptide contained in the venom of the marine snail Conus geographus and blocks the acetylcholine receptor at the neuromuscular junction.

In order to make peak assignments, so-called individual and sequential assignments were carried out with two dimensional NMR of COSY and NOESY. The distance constraints were obtained by the translation of intensities of proton-proton NOE's which were measured by NOESY with various mixing times. The translation was done by three ways which stand on rigid, uniform averaging and threshold value models respectively. Obtained distance constraints were systematically treated by a distance geometry algorithm. The algorithm which we used here consists of the determination and minimization of a proper target function. Only dihedral angles are used as variables in this function to reduce memory space and calculating time in the computer. This algorithm is coded DADAS ( Distance Analysis in Dihedral Angle Space ). In order to define the conformational space satisfying experimentally obtained distance constraints, calculations were repeated from different initial conformations which were generated randomly.

CLASSIFICATION OF INTERACTIONS OF HUMAN SERUM ALBUMIN WITH  
LIGAND MOLECULES AS STUDIED BY PROTON NMR SPECTROSCOPY

Tetsuya Oida

Research Laboratories, Dainippon Pharmaceutical Co., Ltd.

Suita-shi, Osaka, JAPAN

Interactions of human serum albumin (HSA) with a variety of ligand molecules were studied.  $^1\text{H}$ -NMR spectra of HSA solutions were measured with and without ligands. Difference spectra (ligand presence-absence) showed the type of ligand binding. In non-specific binding (weak interactions), signals of HSA were cancelled out, and only broadened signals of ligand molecules were observed. By contrast, in specific binding (strong interactions), signals from ligand molecules were hardly observed, while signals from HSA showed drastic changes owing to the induced conformational change of HSA.

These allosteric effects observed by  $^1\text{H}$ -NMR spectroscopy are quite useful for investigation of ligand-HSA interactions. Firstly, difference spectral patterns were nearly the same for several ligands which were bound to a common specific site on HSA. Difference spectra of more than thirty kinds of ligand molecules were compared with difference spectra of two typical ligand molecules on the basis of characteristic peaks for each type: one is ibuprofen, the other is warfarin. Secondly, interactions of different ligands simultaneously bound to HSA could be investigated. If a difference spectrum of one ligand was altered when another ligand was added, two sites of these molecules were interrelated. In such a way, it was possible to classify binding sites more definitely and to map the binding sites on HSA.

Tryptophan binding was one of the typical examples. D-tryptophan binding was non-specific, while L-tryptophan binding was specifically at the ibuprofen site. Oleic acid addition to HSA weakened binding of both isomers, which resulted in non-specific binding of both isomers. However, the difference spectra for oleic acid were not affected by the addition of tryptophan, which means oneway influence in two-ligand binding.

# COMPUTER SIMULATION PROGRAM FOR PROTON RELAXATION IN PROTEINS

Susumu Shibata and \*Kazuyuki Akasaka

Department of Biochemistry, Kinki University School  
of Medicine, Osaka, and \*Department of Chemistry,  
Faculty of Science, Kyoto University, Kyoto, Japan

Proton spin relaxation can be a useful tool to determine the conformation and dynamics of a protein molecule in solution. So far, however, only a limited class of information of proton spin relaxation has been utilized for this purpose. In an effort to extend the utility of proton spin relaxation in the study of the structure and dynamics of a protein, a computer program for longitudinal relaxation of protons in protein molecules in solution has been developed in our laboratory.

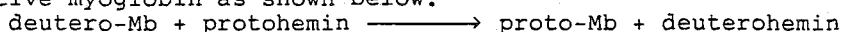
The program takes into account dipolar couplings between protons based on given coordinates (usually obtained from Protein Data Bank) and a single correlation time is usually assumed. At present, the number of protons which are directly taken into account for calculation is limited by the size of a core memory to 300-500, so that for most proteins only a part of the molecule can be handled at one time. This program is available for the following types of relaxation measurements, i.e., non-selective excitation, selective excitation, cross-saturation, and NOE experiments. Some typical examples of the use of this program will be given. (see also lecture E9 of this conference.)

THE MECHANISM AND THE PRESSURE DEPENDENCE OF HEME REORIENTATION  
AND HEME EXCHANGE REACTION OF HEMOPROTEINS

Koichiro Ishimori, Masahiro Aoki and Isao Morishima

Division of Molecular Engineering,  
Graduate School of Engineering,  
Kyoto University, Sakyo-ku, Kyoto 606, Japan

Toward further understanding of the interaction between heme and globin in hemoproteins, we present here some results of proton NMR studies of heme-reorientation and the heme-exchange reaction for the reconstituted myoglobin and hemoglobin by utilizing high pressure NMR spectroscopy. The recent studies have shown that major structural heterogeneity exists for these reconstituted proteins, with the two heme orientations, the native and disordered forms, differing in their heme orientation by  $180^\circ$  about the  $\alpha$ - $\gamma$ -meso axis. The disordered form reorients in time to the native form. Another interesting reaction representing the dynamical structure of the protein is the heme-exchange reaction in which deuterohemin embedded in the reconstituted myoglobin is exchanged with protohemin to form native myoglobin as shown below.



As Figure 1 shows, the heme reorientation reaction and the heme exchange reaction for the reconstituted myoglobin are accelerated under high pressure. The apparent activation volume at 1 atm for both reactions are estimated as ca.  $-160 \text{ \AA}^3$ . However, it is also evident that the rate of heme-reorientation reaction retarded at higher pressure, whereas the plot of  $\ln k$  vs. pressure for the heme-exchange reaction is linear at any pressure. These reactions could be explained by the scheme depicted in Figure 2 in which the heme-reorientation may proceed through the path (3) (heme-reorientation in the hydrophobic protein cage) and the heme-exchange reaction through the path (2). This may be responsible for quite a different feature of pressure dependence of heme-reorientation and heme-exchange reaction rates.

It is also to be noted that the heme-exchange reaction proceeded even in native myoglobin and hemoglobin in the presence of large excess of the modified heme. This observation indicates that the large conformational fluctuation takes place in the path (2) so as to induce the displacement of heme even in the stable native protein.

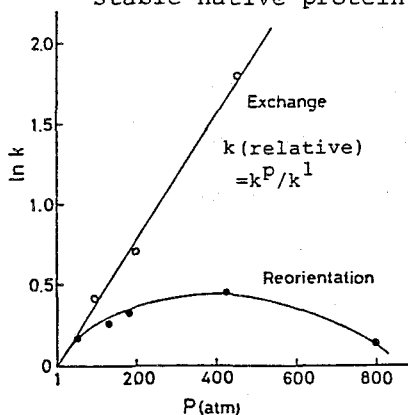


Figure 1.

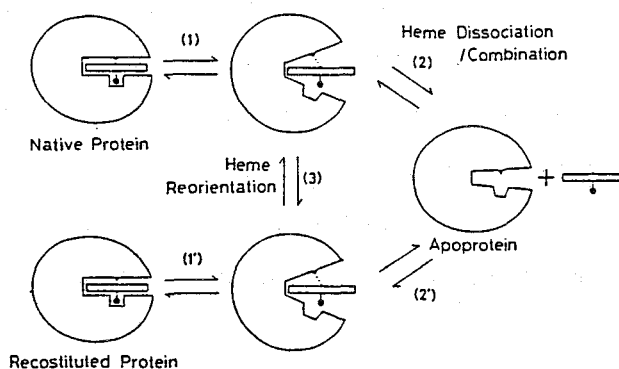


Figure 2.

## PHOTO CIDNP STUDIES OF IMMUNOGLOBULINS

Fumiaki Hayashi, Yoshimasa Kyogoku, Satoshi Endo\*,  
and Yoji Arata\*

Institute for Protein Research, Osaka University and

\* Faculty of Pharmaceutical Sciences, University of Tokyo

Immunoglobulin G (IgG) consists of two identical Fab and one Fc regions. The Fc region of IgG plays an important role for activation of effector function, e.g., activation of complement system. Fc is classified into four subclasses according to the difference of its amino acid sequence. There are slight differences in their functions. To investigate the difference from the structural aspects we assigned all of the CIDNP signals and some other signals in normal spectrum. Discrepancy between the CIDNP intensity and accessible surface area obtained from X-ray data were found. We will discuss the problem, and then mention about the comparison of IgGs in different subclasses.

To find the origin of the discrepancy we checked three contributions to CIDNP intensity one by one; 1) accessibility to the site from which an electron or H atom is abstracted (aromatic OH or NH group); 2) accessibility to the whole aromatic ring; 3) hydrogen bonding. By comparing them with NMR data the above discrepancy became to be explainable to some extent. We have further investigated the spectral difference of IgGs in different subclasses. In the homogated irradiation spectra we newly found Phe 296 and the other two signals specific to a subclass (maybe Tyr). On the basis of these assignments we investigated the difference of the environment of the residues by using the informations on the CIDNP intensity, spin diffusion rate, and chemical shift deviation. The results showed that the differences in the spectral pattern of subclasses came from the residues around the amino acid substitution sites and in the contact region between the CH2 and CH3 domains. It is suggested that there exists a difference in quaternary structure among subclasses.

NMR STUDY OF PHILOSAMIA CYNTHIA RICINI SILK FIBROIN STRUCTURE  
IN SOLUTION

Tetsuo Asakura, Makoto Demura, and Hitoshi Kashiba  
Department of Polymer Engineering, Faculty of Technology,  
Tokyo University of Agriculture and Technology,  
Koganei, Tokyo, Japan

Liquid silk from P.c.ricini is a protein whose major amino acid residues are alanine, glycine, serine and tyrosine. The most striking characteristic of the conformation is the presence of  $\alpha$ -helical portion (ca. 30 %) which consists of the  $-(\text{Ala})_n$ -sequence.

In this study,  $^{13}\text{C}$  NMR spectroscopy has successfully applied to the conformational characterization and also the conformation transition from  $\alpha$ -helix to random coil. Peak doublings in the  $^{13}\text{C}$  NMR were observed not only for the  $\text{C}_\alpha$  and carbonyl but also for the  $\text{C}_\beta$  carbons of the alanine residue. In addition, the low-field peaks of the  $\text{C}_\alpha$  and carbonyl carbons shift upfield 1.0 and 1.5 ppm, respectively, while the upfield peak of the  $\text{C}_\beta$  carbon shifts downfield 0.5 ppm as the temperature is increased from  $-5$  to  $+50$  °C. However, other peaks show no temperature dependence. In order to analyse these spectral behavior quantitatively, the carbonyl peak was simulated on the basis of the statistical thermodynamic analysis by Bixon-Scheraga-Lifson.

At first, the averaged number of the  $-(\text{Ala})_n$ - sequence in P.c.ricini silk fibroin was determined 22 from the  $^1\text{H}$  NMR spectra of the residue obtained from the hydrolysis of the silk fibroin.

Secondary, the helicity of every residue of the  $-(\text{Ala})_{22}$ - was calculated with statistical thermodynamic analysis according to Bixon-Scheraga-Lifson and then, the simulation for the carbonyl resonance region was performed assuming Gaussian. The asymmetric shape of the main h peak and appearance of the  $h^*$  peak, which was assigned to the terminal residue of the  $-(\text{Ala})_{22}$ -, were successfully reproduced.

Temperature dependence of the Ala carbonyl resonance was also simulated as functions of A (linewidth) and w (statistical weight of intramolecular hydrogen bond). The observed high field shifts of the h and  $h^*$  peaks were reproduced in terms with decrease in the value of w. Thus, the helix-coil transition occurred in P.c.ricini silk fibroin protein is interpreted very well on the basis of Bixon-Scheraga-Lifson theory.



# CHARACTERISTICS OF PROTEIN HYDRATION BY $^2\text{H}$ NMR

Naofumi HANAFUSA

Institute of Low Temperature Science, Hokkaido University

It was examined that the alteration of the extents of the hydration and the interaction of hydration water with protein molecule varying temperature on the unfrozen water of protein solution in  $\text{D}_2\text{O}$  by  $^2\text{H}$  NMR. The results were compared with them obtained by  $^1\text{H}$  NMR.

The crystallized proteins were dissolved in 99.7 %  $\text{D}_2\text{O}$ . The  $^2\text{H}$  NMR measurements were carried out by a JEOL FX100 FTNMR equipped  $^2\text{H}$  probe and temperature controlling unit. The amount of unfrozen water of  $\text{D}_2\text{O}$  in the protein solution was estimated by comparing of  $^2\text{H}$  signal areas with that of standard  $\text{D}_2\text{O}$  solution. The relaxation measurements of  $T_1$  were made by inversion recovery method.

The extents of the hydration, the amounts of unfrozen water, were decreased by lowering the temperature and retained similar values in the region between  $-10$  to  $-30^\circ\text{C}$ . They were decreased further below this region. The region, of monolayer hydration, was shifted to higher temperature about  $5$  to  $10^\circ\text{C}$  than the results in  $\text{H}_2\text{O}$ . The hydration values, the amounts of unfrozen water in this region, were similar or slightly decreased as compared with the results by  $^1\text{H}$  NMR.

For the estimation of molecular correlation time  $\tau_c$  by quadrupole relaxation, the extent of the interaction between hydration water and protein molecule, most reports used the value of  $215$  KHz for the quadrupolar coupling constant obtained from  $\text{D}_2\text{O}$  ice or liquid crystal. It could be obtained the value of the coupling constant using minimum value on the relaxation curve against temperature under limited condition ( $\omega_0\tau_c \ll 1$ ) based on the equation of quadrupole relaxation.

Actually the estimated value of the constant was about  $60$  KHz. Using both values of measured and reported, the correlation times of unfrozen water of  $\text{D}_2\text{O}$  in protein solution at optional temperatures were estimated approximately from the experimental results, respectively. The values of  $\tau_c$  were greater about  $10$  times at same temperature than in  $\text{H}_2\text{O}$ . Though the coupling constant obtained here was very small than reported one, it could be well explained the experimental results.

## DEUTERIUM NMR STUDY OF ORIENTED DNA FIBERS

Heisaburo Shindo, Yukio Hiyama\* and D.A. Torchia\*  
Tokyo College of Pharmacy, Hachioji, Tokyo Japan and \*Bone  
Research Branch, National Institute of Dental Research,  
NIH, Bethesda, MD USA.

Solid-state  $^2\text{H}$  NMR spectra were measured as a function of relative humidity for non-oriented DNA films and oriented DNA fibers deuterated at C8 carbons of the purine bases. The line-shape analyses of the quadrupole echo spectra from oriented DNA fibers demonstrated that the purine base planes of the A form of DNA were tilted by about  $70^\circ$  relative to the helix axis, and that the base planes of the B form varied significantly, although they were, on average, perpendicular to the helix axis. These results were generally consistent with the x-ray fiber diffraction studies and the single crystal structure of oligonucleotides.

Analyses of  $^2\text{H}$  relaxation times,  $T_1$  and  $T_2$  from oriented fibers and non-oriented DNA films, showed at 79% RH that the orientation of the base planes fluctuated about an axis normal to the helix axis with a correlation time,  $\tau_C = 3.6 \times 10^{-8}$  s and amplitude of  $8.5^\circ$ . The correlation time of the base plane fluctuation was  $1.5 \times 10^{-8}$  s and amplitude was  $13.5^\circ$  at 92% RH. In addition, at 92% RH but not at 79% RH, the base plane re-oriented slowly,  $\tau \sim 10^{-6}$  s, about the helix axis, through an rms angle of ca.  $30^\circ$ .

The above results were compared with the results obtained previously by  $^{31}\text{P}$  NMR studies.

## TWO DIMENSIONAL AND ZERO FIELD NMR OF ORIENTED MOLECULES

M. Gochin, D. Hugi-Cleary, M. Luzar, K. Schenker, A. Thayer, and A. Pines

University of California, Berkeley, CA 94720, USA

There have been some recent advances in multiple pulse techniques both in high field NMR and in zero field NMR. Most applications in our laboratory have been in solids but these techniques turn out to be very useful in other phases as well. As an example liquid crystals can be studied free of the perturbing effect of the magnetic field on the ordered fluid. We shall describe some theoretical and experimental NMR developments in this area.

DIPOLAR SASS NMR SPECTROSCOPY:  
SEPARATION OF DIPOLAR POWDER PATTERNS IN ROTATING SOLIDS

T. Terao, T.Nakai, H.Miura and A.Saika

Department of Chemistry, Faculty of Science  
Kyoto University, Kyoto 606, Japan

A novel means that we recently developed will be discussed, which allows us to separately observe heteronuclear direct and indirect couplings at individual chemically inequivalent sites in polycrystalline and amorphous solids. This is a two-dimensional sample-spinning NMR method involving switching the spinning axis on and off the magic angle during the course of the experimental sequence.

What are observed by the SASS method are not spinning sidebands but powder patterns; consequently by using this method even small dipolar couplings and the spectral fine structures due to molecular motions, remote spins, methylene bond angles  $\angle\text{HCH}$ , etc. can be observed clearly in comparison with methods based on observation of spinning sidebands. The calculated and experimental dipolar SASS spectra demonstrate that the spectral line shape allows determination of bond lengths and angles, and the magnitude and absolute signs of the indirect coupling constants, provides information on molecular dynamics, and renders help in spectral assignment. Among them, examination of dynamic fine structures of a molecule is a very important application of dipolar SASS spectroscopy. Studies of  $\beta$ -quinol-methanol clathrate and urea-trans-4-octene clathrate ensure that this experiment is very useful for selectively obtaining local information in a complex molecular system.

Extensions of dipolar SASS spectroscopy will be also discussed, including separation of homonuclear dipolar powder patterns.

# Frequency Switched Inversion Pulse and its Application to Broadband Decoupling

Toshimichi Fujiwara, Kuniaki Nagayama

Biometrology Lab, JEOL LTD. Nakagami, Akishima, Tokyo

A series of broadband inversion pulses for two level system were constructed by the use of frequency and phase switching. They were applied to broadband spin decoupling. A systematic procedure to design these pulse sequences will be shown together with experimental and numerical results.

At the first step, the broadband inversion pulses with rapid frequency switching were designed. They are approximately made of a few  $180^\circ$  pulses which are different in frequency of about  $1.5 \times B_1$ , where  $B_1$  indicates strength of r.f. field. The frequency differences and pulse widths were refined numerically under the constraint of symmetry about offset frequency. The operative frequency range of these pulses is about  $1.2 \times B_1 \times n$ , where  $n$  is the number of frequencies used, or the number of  $180^\circ$  pulses in the sequence. This class of pulses is thought to belong to a frequency sweep, but doesn't satisfy the adiabatic fast passage condition. At the second step, the performance and the tolerance of inhomogeneity of  $B_1$  field were improved by the phase cycling\* of  $0^\circ, 150^\circ, 60^\circ, 150^\circ, 0^\circ$ .

Finally  $0^\circ$  pulses i.e. decoupling pulses were constructed from these improved inversion pulses by the phase cycling of MLEV.

\* R.Tycko, A.Pines, Chem.Phys.Letters 111, 462 (1984)

DETERMINATION OF THE  $^{14}\text{N}$  QUADRUPOLE COUPLING TENSORS IN A SINGLE  
CRYSTAL OF L-HISTIDINE HYDROCHLORIDE MONOHYDRATE  
BY NMR SPECTROSCOPY

C.A. McDowell, A. Naito\*, D.L. Sastry, and K. Takegoshi

Department of Chemistry, University of British Columbia,  
2036 Main Mall, Vancouver, British Columbia V6T 1Y6, Canada

\*Department of Chemistry, Faculty of Science, Kyoto University,  
Sakyo-ku, Kyoto 606, Japan

It is of considerable interest to study the  $^{14}\text{N}$  quadrupole coupling tensors of the nitrogen nuclei in the imidazole ring if we are to understand the chemical nature of imidazole compounds like histidine, because those nuclei play an important role in the structure of biological molecules. Quadrupole coupling tensor data can provide information about the nature of chemical bonding since the magnitudes of the tensor are very sensitive to the charge distributions on the quadrupole nuclei.

The  $^{14}\text{N}$  quadrupole coupling tensors of the  $\text{NH}_3^+$ , N2 and N3 nitrogen in a single crystal of l-histidine hydrochloride monohydrate were determined using proton enhanced  $^{14}\text{N}$  NMR with high power proton decoupling. The signs of the  $^{14}\text{N}$  quadrupole coupling constant,  $e^2Qq/h$ , for the three chemically distinct nitrogen nuclei could be determined by analysing the line shapes of the  $^{13}\text{C}$  CP-MAS NMR signals of the C2, C4 and C6 carbon nuclei which are directly bonding to one of those nitrogen nuclei. The  $^{14}\text{N}$  quadrupole coupling constants including their signs and the asymmetry parameters,  $\eta$ , were evaluated to be ( $e^2Qq/h=1.147\text{MHz}$ ,  $\eta=0.189$ ), ( $e^2Qq/h=1.465\text{MHz}$ ,  $\eta=0.268$ ) and ( $e^2Qq/h=-1.287$ ,  $\eta=0.946$ ) for the  $\text{NH}_3^+$ , N2 and N3 nitrogen nuclei, respectively. The direction of the largest principal axis of the  $^{14}\text{N}$  quadrupole coupling tensor for the  $\text{NH}_3^+$  nitrogen nucleus is almost parallel to the N1-C2 bond direction, while that for the N2 nitrogen nucleus makes an angle of  $33^\circ$  with the N2-C4 bond direction in the C4-N2-C5 plane, and for the N3 nitrogen nucleus it is perpendicular to the C5-N3-C6 plane. The difference between the  $^{14}\text{N}$  quadrupole coupling tensors of N2 and N3 nitrogens, can be attributed to the difference in the hydrogen bonding at those two sites.

# $^{13}\text{C}$ NMR Spectra of Liquid Crystalline Compounds.

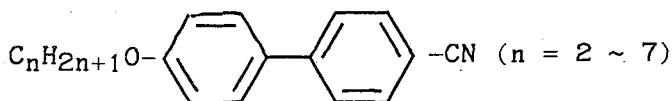
## 1. 4'-Alkoxy-4-biphenylcarbonitriles.

Kikuko Hayamizu, Masaru Yanagisawa, and Osamu Yamamoto

National Chemical Laboratory for Industry,

Tsukuba Research Center, Ibaraki 305

Nematic liquid crystalline substances, 4'-alkoxy-4-biphenyl carbonitriles,



have been studied by  $^{13}\text{C}$ NMR in the solid, nematic, and isotropic phases. The spectra in the isotropic spectra for these compounds are similar to those in the  $\text{CDCl}_3$  solutions. In the nematic state, the quaternary carbons of the benzene rings show the signals in the lower field, while the nitril carbon appears in the higher field about 20 to  $-20$  ppm from TMS, depending on the temperature. The signals for the aromatic carbons are fairly sharp, while the alkoxy side chain carbons show very broad signals. In the solid state high resolution  $^{13}\text{C}$  NMR of these liquid crystals, the alkoxy and quaternary carbons show sharp signals, while protonated aromatic carbons give broad signals. The  $^{13}\text{C}$  shifts in the solid state are almost similar to those in the isotropic state. At the same time, when the number of alkyl carbons is even, the  $^{13}\text{C}$  signals show a doublet for some of the peaks, which indicates that some specific interaction between the molecules exists in the solid state. We also observed the  $^{13}\text{C}$  relaxation time,  $T_1$ , in the solid state, which clearly indicates that molecular motions are quite different at the aromatic rings and side chains.

$^{63}\text{Cu}$  MAS NMR of Mixed Crystals of  $\text{CuY}_x\text{Z}_{1-x}$  (Y=Cl or Br; Z=Br or I) and  $\text{Cu}_x\text{Ag}_{1-x}\text{I}$

Kazunaka Endo, Kyonosuke Yamamoto, Makoto Okaji, Kenzo Deguchi,<sup>+</sup> Kazuhiro Matsushita<sup>+</sup> and Teruaki Fujito<sup>+</sup>

R&D Laboratories for Photo Materials, Mitsubishi Paper Mills, LTD. Nagaokakyo, Kyoto and <sup>+</sup>NMR Application Laboratory, Scientific Instrument Division, JEOL LTD. Tokyo

$^{63}\text{Cu}$  MAS NMR and X-ray diffraction methods have been used to perform the structure analysis of mixed crystals,  $\text{CuY}_x\text{Z}_{1-x}$  and  $\text{Cu}_x\text{Ag}_{1-x}\text{I}$ . For the mixed crystals, we have produced complete solid-solution and a core-shell type of crystal: The one is prepared by the melt-annealing method and the other by a conversion process in aqueous suspension by using solubility difference between metal halides. In the 23rd NMR Symposium, we presented an availability for structure analysis of mixed crystals,  $\text{CuY}_x\text{Z}_{1-x}$ , by use of the both methods. Here, we will give a simulation for  $^{63}\text{Cu}$  MAS NMR spectra of the mixed crystals,  $\text{CuCl}_x\text{Br}_{1-x}$  and  $\text{CuBr}_x\text{I}_{1-x}$ , and provide the extended study of mixed crystals.

The simulation was performed by solving a nonlinear recurrence equation which is held between observed and assumed spectra for Gaussian lineshape of five tetrahedral structure species,  $\text{Cu-Y}_4$ ,  $\text{Cu-Y}_3\text{Z}$ ,  $\text{Cu-Y}_2\text{Z}_2$ ,  $\text{Cu-YZ}_3$  and  $\text{Cu-Z}_4$ , with Gauss-Newtonian methods. The simulation spectra correspond fairly well to observed ones.

Both MAS NMR and X-ray diffraction methods have also been used to discriminate whether  $\text{CuY}_x\text{Z}_{1-x}$  mixed crystals which were prepared by a conversion process in aqueous suspension in a range of 20 to 80 °C are a nearly complete solid-solution, or core-shell type. Thus, in the preparation below 40 °C,  $\text{CuCl}_x\text{Br}_{1-x}$  is a core-shell type of crystal, and  $\text{CuBr}_x\text{I}_{1-x}$  becomes the same type below 70 °C.

For  $\text{Cu}_x\text{Ag}_{1-x}\text{I}$  crystals, we have synthesized complete solid-solution and a core-shell type of crystal.  $^{63}\text{Cu}$  signals in the complete solid-solution shifted around tens of ppm, relative to solid CuI, while the signal in a core-shell type of crystal did not almost shift.



Nuclear Magnetic Resonance of B22-26 Pentapeptide and the  
Methyl Ester of B23-25 Tripeptide of insulin  
Qing-luo Shi, You-min Feng and Zi-xian Lu  
Shanghai Institute of Biochemistry, Academia Sinica  
320 Yue-yang Road, Shanghai 200031, China

It was previously reported that the affinity of insulin with its receptor could be promoted by insulin B22-26 fragment, RGFFY, or inhibited by the methyl ester of insulin B23-25 fragment, GFF-OMe. Proton magnetic resonance studies of two peptides in d6-DMSO solution were undertaken to explore their structure-function relationships.

J-connections of each residue were acquired through two-dimensional correlated spectroscopy (COSY). Assignment ambiguities arising due to the overlap of aromatic side chain resonances were resolved by double quantum two-dimensional correlated spectroscopy. Though small peptides were often shown to be poor samples for two-dimensional NOE spectroscopy (NOESY) because of their unfavorable correlation times and/or conformational averaging, satisfactory NOESY spectra of these two peptides were obtained by the elaborate selection of mixing time, randomization value, and window function. Relayed NOESY and double quantum NOESY which have been developed to resolve ambiguities present in conventional NOESY spectra were also attempted. Complete sequential assignment of the two peptides were acquired thereupon.

Various NMR approaches were employed to get the information about the conformations and dynamic of both the backbone and side chains. Attentions were focused on the comparison of chemical shifts, vicinal coupling constants, chemical exchange, and spin-lattice relaxation times of the GFF portions of the two peptides. Thus it appears that interactions between residues in RGFFY are stronger than those in GFF-OMe, and that RGFFY assumes more rigid conformation than GFF-OMe. Implications for their function-conformation relationships were discussed.

Mechanism of Activation of Hormone-Sensitive GTP-Binding  
Regulatory Protein by F<sup>-</sup> ion

Tsutomu Higashijima and Masatsune Kainosho\*

Department of Biophysics and Biochemistry, Faculty of Science,  
University of Tokyo, \*Department of Chemistry, Faculty of  
Science, Tokyo Metropolitan University, Tokyo, Japan.

Members of a family of guanine nucleotide-binding regulatory proteins (G-proteins) serve as membrane-bound transducers, that couple the activation of receptor by extracellular ligands to the regulation of intracellular macromolecular effectors. Such a multiprotein complex has been studied extensively in hormone-sensitive adenylyl cyclase system.

The G-proteins that have been purified to date (G<sub>s</sub>, G<sub>i</sub>, transducin and G<sub>o</sub>) are oligomers of three types of polypeptides, namely a guanine nucleotide-binding subunit (G<sub>α</sub>), a polypeptide of about 35 kDa (G<sub>β</sub>), and a peptide of 5-10 kDa (G<sub>γ</sub>). The G<sub>α</sub> subunits vary in size from 39 kDa to 52 kDa, but they are clearly homologous.

G-proteins (G<sub>α</sub> subunit) are in inactive form when GDP is bound. Interactions of G-proteins with activating ligands (GTP, unhydrolyzable GTP analog such as GTPγS, and AMF (Al<sup>3+</sup>, Mg<sup>2+</sup>, and F<sup>-</sup>)) cause characteristic changes in their structure and function of G-proteins. GTP activates G-proteins tentatively, since bound GTP is hydrolyzed to GDP by G-proteins. On the other hand, AMF as well as GTPγS activates G-proteins persistently. It is quite interesting why AMF activates G-proteins as well as GTPγS. Here we reports the molecular mechanism of activation of G<sub>oα</sub> subunit by F<sup>-</sup> ion by using <sup>19</sup>F- and <sup>32</sup>P-NMR spectroscopy.

<sup>19</sup>F-NMR spectrum of G<sub>oα</sub> subunit in the presence of AMF showed two peaks at -10 ppm and -29 ppm. In the absence of G-protein, only the peak at -10 ppm was observed. Accordingly the peak at -29 ppm was assigned to F<sup>-</sup> bound to G-protein. The concentration of the F<sup>-</sup> ion bound to G-protein was calculated to be ca. three times as that of G-protein; three F<sup>-</sup> ions bind to one G-protein α subunit. For the observation of the resonance signal of bound F<sup>-</sup> ion, Mg<sup>2+</sup> and Al<sup>3+</sup> were indispensable.

The <sup>31</sup>P chemical shifts of bound GDP (-2 and -8.5 ppm for α and β phosphate, respectively) of G<sub>oα</sub> were significantly different from those of free GDP (-6 and -10 ppm). The addition of AMF caused remarkable higher field shift (6 ppm) only of the β phosphate peak.

These observations, in combination with the fluorescence analysis, showed that G<sub>α</sub>-bound GDP is required for the activation of G<sub>α</sub> by AlF<sub>3</sub> and that the AlF<sub>3</sub> mimics the γ phosphate of GTP.

#### Acknowledgement

We are grateful to Professors T. Miyazawa and A. G. Gilman for their generous discussions and encouragement.

## 2D NMR STUDIES OF THE SPECIFICITY OF DIHYDROFOLATE REDUCTASE

GORDON C.K. ROBERTS

Department of Biochemistry,  
University of Leicester,  
Leicester, U.K.

Dihydrofolate reductase ( $M_r$  18,300) is the target for a number of clinically useful drugs, including methotrexate and trimethoprim. We have been using nmr to study the molecular basis of the specificity this enzyme shows in binding small molecules.

By a combination of 2D (COSY, RELAY, NOESY) spectra, selective deuteration and semi-quantitative use of crystallographic information, we have assigned  $^1\text{H}$  resonances from about 25% of the residues of the protein. Using these assigned resonances as 'reporters', we can begin to define the conformational changes which accompany ligand binding, and to describe the differences in mode of binding among a series of closely related inhibitors.

It has been established that the substrate, folate, and the closely related inhibitor methotrexate bind quite differently to the enzyme. By a combination of  $^1\text{H}$ ,  $^{13}\text{C}$  and  $^{15}\text{N}$  nmr, we have characterised the conformational equilibria in the enzyme-folate and enzyme-folate-NADP<sup>+</sup> complexes and shown that the substrate can bind in 'productive' and 'non-productive' modes, while the inhibitor binds exclusively in the 'non-productive' mode.

Nmr studies of dihydrofolate reductase containing single amino-acid substitutions, produced by oligonucleotide-directed mutagenesis, will also be discussed.

A NEW STRATEGY TO DETERMINE THE SOLUTION STRUCTURE OF  
A PROTEIN USING  $^{13}\text{C}$ -NMR SPECTROSCOPY

- A PROTEIN PROTEINASE INHIBITOR SSI -

Masatsune Kainosho, Hiromasa Nagao, Atsuhiko Hirose

Department of Chemistry, Faculty of Science, Tokyo Metropolitan  
University, Setagaya-ku, Tokyo, Japan

The carbonyl carbon resonances of SSI have been classified into the subspectra representing the each type of 113 amino acid residues which consist of a polypeptide chain of the subunit. A carbonyl carbon NMR region of SSI reconstructed from a complete set of the subspectra fit perfectly well with that of the natural abundant  $^{13}\text{C}$  NMR spectrum. During these several months we have made a fair progress in the site-specific assignment of those classified carbonyl subspectra, and we are now very confident to be able to establish *the complete assignment* of the back-bone carbonyl NMR signals within a few years. With this new situation in mind, we have urged to explore a general technique to extend the carbonyl assignments to all of the side-chain groups.

In a preliminary result for the two Lys residues in SSI, we clearly showed that the most powerful technique for such purpose is undoubtedly the use of uniformly  $^{13}\text{C}$  labeled amino acids (The 24th NMR Symposium Japan, Tsukuba, 1985). We have applied this method to the nine Leu residues, for which assignment of the carbonyl resonances have been almost established. A general strategy using the site-specifically assigned various NMR resonances for studying the larger proteins for which most of the existing two-dimensional techniques fail to be applied will be discussed, if the allotted time allows us to do it.

BINDING MODES OF INHIBITORS AND A SUBSTRATE ANALOG TO  
RIBONUCLEASE T<sub>1</sub> AS STUDIED BY NMR

Fuyuhiko Inagaki, Yasuyuki Shibata, Ichio Shimada  
and Tatsuo Miyazawa

The Tokyo Metropolitan Institute of Medical Science, 18-22, Honkamagome 3-chome, Tokyo 113 and Department of Biophysics and Biochemistry, Faculty of Science, University of Tokyo, Bunkyo-ku, Tokyo, 113 Japan.

Ribonuclease T<sub>1</sub> (RNase T<sub>1</sub>) is an acidic protein isolated from Takadiastase, a commercial product of *Aspergillus oryzae*. RNase T<sub>1</sub> specifically cleaves ribonucleic acid chains at guanylic acid residues in contrast to the pyrimidine specificity of bovine pancreatic ribonuclease A. Rigorous recognition of guanine base by RNase T<sub>1</sub> is a typical example of RNA-protein interactions. Recently, the crystal and molecular structures of the complex of RNase T<sub>1</sub> and guanosine 2'-phosphate (2'-GMP) have been elucidated by X-ray analysis. On the basis of such structures, the proton NMR spectra of RNase T<sub>1</sub> in aqueous solution may now be analyzed in detail.

In the present study, we have analyzed the dependence of chemical shifts of high field shifted methyl proton resonances of RNase T<sub>1</sub> on the binding of inhibitors and a substrate analog, 2'-deoxy-2'-fluoroguanlyl-(3'-5')-uridine (G<sub>fp</sub>U). These methyls have been classified into two groups; one is located at the recognition site of the guanine base and the other, at the binding site of the phosphate group. Moreover, the limiting shifts of those methyl proton resonances are similar, suggesting that the relative orientation of the inhibitors and the analog to RNase T<sub>1</sub> is nearly the same. From the analyses of nuclear Overhauser effects for the pair of H8 and H1' protons, together with the analyses of the vicinal coupling constants for the pair of H1' and H2' or H1' and F2', the conformation of the guanosine moiety as bound to RNase T<sub>1</sub> was found to be C3'-endo-syn for 3'-GMP, 2'-GMP and G<sub>fp</sub>U. The productive binding to RNase T<sub>1</sub> probably requires the syn form of the guanosine moiety of RNA substrates.

## COMPUTER SIMULATION OF SPIN DIFFUSION IN PROTEINS

Kazuyuki Akasaka and Susumu Shibata\*

Department of Chemistry, Faculty of Science, Kyoto

University, Kyoto and \*Department of Biochemistry, School of  
Medicine, Kinki University, Osaka

In order to further clarify the relationship between spin diffusion and the gross conformation of a protein in solution, time dependence of cross saturation in the proton NMR spectrum was computer-simulated using the program developed in our laboratories (cf. lecture 15 of this conference). This paper reports results of simulation mainly in Streptomyces subtilisin inhibitor (SSI) for experiment at 400 MHz. The calculation was performed based on coordinates given by x-ray diffraction (Y. Mitsui et al., J. Mol. Biol. 131, 697, 1979) under the assumption of isotropic rotational diffusion, neglecting internal motions. However, the three-site jumps for methyl protons and the  $180^\circ$  jumps of tyrosine and phenylalanine rings were considered to average relaxation matrices of respective protons. The result of calculation clearly indicates that upon saturation of the resonance of the core protons, saturation prevails in the entire spectral region after 2 seconds, but that the signals from the segment involved in binding to the protease, subtilisin BPN', is almost unaffected. Similar result was obtained when some of the methyl protons in the protein core were chosen for initial saturation, in qualitative agreement with experiment (K. Akasaka, J. Magn. Reson. 51, 14, 1983). The present result also indicates that "the geometrical factor" (or the exposure of segment) can be a decisive factor in determining selectiveness of spin diffusion.

PROTON NUCLEAR MAGNETIC RESONANCE STUDIES OF PROTEINS OF  
IMMUNOLOGICAL INTEREST

W.Ito, S.Endo, Y.Muto, M.Nishimura, N.Higashi, and Y.Arata  
Faculty of Pharmaceutical Sciences, University of Tokyo  
Hongo, Tokyo 113, Japan

N.Sakato and H.Fujio  
Department of Immunology, Research Institute for Microbial  
Diseases, Osaka University Medical School  
Suita, Osaka 565, Japan

F.Hayashi and Y.Kyogoku  
Institute for Protein Research, Osaka University  
Suita, Osaka 565, Japan

Proton nuclear magnetic resonance has been extensively used for the elucidation of molecular structural basis of biological functions of proteins of immunological interest.

1. Flexibility of IgG molecules and its biological significance: Spin diffusion has been observed to discuss the biological significance of the mosaic structure that constitutes the hinge part of the molecule.

2. Interactions between Fc and staph protein A: The pKa values of histidine residues, which exist in the Fc and protein A, were determined on the basis of NMR titration data and used for the calculation of the electrostatic potential profiles for the two interacting surfaces. Possible mechanisms for the pH dependent interactions between these two proteins will be discussed on the basis of the pattern of the electrostatic potential profiles.

3. Mode of interactions between antigen and antibody: Interactions between hen egg white lysozyme (HEL) and a monoclonal antibody raised against it were studied. A peptide fragment P<sub>17</sub>'<sup>1</sup>, which corresponds to one of epitopes on the HEL molecule, and the antibody were used for the analyses of the mode of the antigen-antibody interactions. Intermolecular transferred nuclear Overhauser effect was observed and analyzed. The results obtained will be discussed in terms of the potential profiles that are similar to those used for the analyses of the Fc-protein A interaction.

4. Photo-CIDNP analyses of the surface structure of IgG molecules: A variety of IgG molecules of subclasses 1-4 have been used for the assignments of His, Tyr, and Trp residues that exist on the surface of the IgG molecules. Possible modes of interactions between IgG and Clq will be briefly discussed.

5. Structure and functions of the third component of complement C3: A method of spin diffusion has been used along with CPase/difference spectroscopy for the analyses of the conformation of the segment intervening C3a and C3b. Similarities and differences between C3 and alpha-2-macroglobulin will also be discussed.

## PROTEIN STRUCTURE AND DYNAMICS BY NMR

Stanley J. Opella  
Department of Chemistry  
University of Pennsylvania  
Philadelphia, Pennsylvania 19104 U.S.A.

The time-average (structure) and time-dependent (dynamic) properties of proteins can be described with solid-state and solution NMR methods. Structure determination by solid-state NMR relies on measurements of orientations of molecular axes relative to the direction of the applied magnetic field in single crystal or uniaxially oriented samples. In contrast, structure determination with solution NMR relies on measurements of intramolecular distances. In both cases considerable computational effort is required to translate the experimental data into molecular structures. The amplitudes and directions of molecular motions can be determined through the analysis of motionally averaged powder pattern lineshapes in solid-state NMR, while the frequencies of the motions can be determined from the analysis of relaxation measurements in both solid-state and solution NMR.

The coat protein of the filamentous bacteriophages provides an example of a protein that is well suited for NMR studies and can not be crystallized in either its structural form in the virus particles or its membrane bound form in lipid bilayers or in detergent micelles. Both solid-state and solution NMR are being used in these studies. A variety of nuclei ( $^1\text{H}$ ,  $^2\text{H}$ ,  $^{13}\text{C}$ ,  $^{14}\text{N}$ ,  $^{15}\text{N}$ ,  $^{31}\text{P}$ ) and spin-interactions (dipole-dipole, chemical shift, quadrupole) are available for analysis because of the ability to incorporate stable isotopes into the protein biosynthetically. Comparisons between the two structural and membrane bound forms of the coat protein are particularly interesting because the protein undergoes transitions between the two forms during the viral lifecycle.



TIME-RESOLVED  $^{31}\text{P}$  NMR STUDIES ON ENERGY UTILIZATION ASSOCIATED  
WITH MUSCLE CONTRACTION.

Kazuhiro Yamada, Masaru Tanokura, Yoshihisa Kawano  
and Takaaki Kitano

Department of Physiology, Medical College of Oita,  
Oita 879-56, Japan

During muscle contraction ATPases are activated. Because of the creatine kinase reaction the net results are a decrease in phosphocreatine (PCr) and an increase in inorganic phosphate ( $\text{P}_i$ ). It has been suspected on various grounds that the utilization of ATP continues well after the contraction is over. We have demonstrated this phenomenon, the post-contraction utilization of ATP, using a time-resolved  $^{31}\text{P}$  NMR, and further that the phenomenon is caused by the actomyosin ATPase activity.

We followed essentially the method of Dawson, Gadian & Wilkie (1977), while the signal-to-noise ratio was greatly improved by using many muscles (Yamada & Tanokura, 1983).

The results indicated that 1) a fixed amount of ATP ( $0.3 \text{ mmol Kg}^{-1}$  muscle, which is equal to the myosin content of muscle) is utilized in an early recovery period ( $\approx 4$  min) at  $4^\circ\text{C}$ , in bullfrog and toad sartorius and bullfrog semitendinosus muscles, irrespective of the duration of contraction. 2) The amount of free phosphates (sum of  $\text{P}_i$  + PCr) increases during contraction, and then decreases during the early recovery period. Amounts of ATP and sugar phosphates (SP) do not change in these periods. 3) At  $10^\circ\text{C}$ , this phenomenon disappears, suggesting the rate of the post-contraction utilization of ATP to be steeply dependent on temperature. 4) The post-contraction utilization of ATP disappears at long muscle lengths where actin-myosin interaction can no longer take place. The above results favour the idea that the post-contraction utilization of ATP is a property of actomyosin, and that it may also be related at least partly to unsolved problems in the study of energy transducing mechanism of muscle.

A  $^1\text{H}$ - $^{31}\text{P}$  CROSS-POLARIZATION STUDY ON IN VIVO SYSTEMS.

Hideo Akutsu, Takayuki Odahara\*, Tomitake Tsukihara\*\*  
and Yoshimasa Kyogoku\*

Faculty of Engineering, Yokohama National University,  
Hodogaya-ku, Yokohama, \*Institute for Protein Research,  
Osaka University, Suita, Osaka, \*\*Faculty of Engineering,  
Tottori University, Minami 4-101, Kozancho, Tottori-shi.

High resolution nuclear magnetic resonance spectroscopy of biological system in vivo has been developed rapidly in the last decade. Especially, phosphorus 31 NMR has been widely used for that purpose. The content of phosphorus in biological systems is not so high as proton, carbon and nitrogen, and thus it makes a spectrum simpler. Although phosphorus is located in important substances such as DNA, RNA and membranes, it was impossible to get high resolution spectra of them in vivo because of their extremely broadened signals. We have developed a method to obtain the information on DNA, RNA and membranes in in-vivo systems separately by the use of solid-state  $^{31}\text{P}$  NMR.

As reported in the last meeting, we have succeeded in obtaining the  $^{31}\text{P}$  NMR spectrum of the chicken erythrocyte chromatin in vivo by the cross-polarization method. The spectrum revealed an asymmetric powder pattern with about -156 ppm chemical shift anisotropy at 4 °C, suggesting that DNA takes on a very rigid structure in the nucleus. We have extended this work to a more complex system, bacteria. In the cross-polarization spectrum of marine bacteria Alteromonas espejiana in full growth, only the contributions from large or insoluble molecules such as DNA, RNA and phospholipids can be expected. With a contact time of 3-7 ms, a powder pattern typical for the phosphorus undergoing an axially symmetrical motion was observed, which can be ascribed to phospholipids in membranes. A symmetrical powder pattern was observed for the contact time of 0.1-0.7 ms. In order to characterize the spectrum, isolated ribosomes were also examined. It was concluded that the DNA in A. espejiana does not have such a rigid higher order structure as that the chicken chromatin has. However, a higher order structure formation of nucleic acids in A. espejiana was observed in their fully active growth phase. Thus it turned out that the cross-polarization spectrum can follow the physiological change in a cell in vivo.

## SPATIAL LOCALIZATION TECHNIQUES FOR IN VIVO NMR

Ray Freeman

Physical Chemistry Laboratory, Oxford University,

South Parks Road, Oxford, England

Nuclear magnetic resonance spectroscopy has made a big impact on medical science, principally through magnetic resonance imaging, but more recently by studying the internal chemistry within living organs, the so-called in-vivo spectroscopy. Here the principal problem is to find a method for defining a restricted "sensitive volume" from which the NMR spectrum will be excited, all other NMR signals being suppressed. It is possible to adapt the imaging techniques to do this, using intense switched gradients of the static magnetic field  $B_0$ , but there are important advantages to be gained if  $B_0$  field gradients can be avoided. An alternative scheme is to utilize the intrinsic spatial inhomogeneity of the radiofrequency field  $B_1$  to define the sensitive volume because most of these experiments are performed with a "surface coil" which by its very nature has a very non-uniform  $B_1$  field distribution. The main difficulties with the surface coil technique are to obtain a sufficiently deep penetration into the sample, to define a suitably-shaped restricted volume and to compensate for off-resonance effects so that the same volume is defined for all chemically shifted species. Composite radiofrequency pulses have been used to tackle this last problem.

Pulse sequences have been devised to exploit the fact that the pulse flip angle varies rapidly across the sample and only satisfies the chosen condition  $\beta = \pi$  radians over a limited region of space. Better spatial definition can be achieved by cascading pulse sequences. Encouraging results have been obtained for phosphorus-31 spectra from phantom samples showing excellent spatial discrimination. Even better performance is predicted for a "straddle coil" scheme where there is a radiofrequency coil on each side of the sample, driven with pulses of opposite phase. Fast electronic switching is used and the two coils can be reconnected in series to act as a sensitive receiver coil with good coupling to the entire sample.

Application of  $^1\text{H}$  Biselective  $T_1$  Data on  
Conformational Analyses in Solution

Makiko Sugiura, Torei Sai, Narao Takao, and Hideaki Fujiwara\*  
Kobe Women's College of Pharmacy, Higashinada-ku, Kobe, Japan

\*Faculty of Pharmaceutical Science, Osaka University, Suita,  
Osaka, Japan

At the last symposium, we discussed the stereochemistry of quinidine using  $^1\text{H}$  selective ( $T_1^i(i)$ ), biselective ( $T_1^i(ij)$ ), and nonselective  $T_1$  ( $T_1^i(\text{all})$ ) data, and emphasized the usefulness of biselective  $T_1$ . The extended and systematic method for conformational and/or stereochemical analysis has now been developed, and biselective  $T_1$  values obtained using the pulse sequence shown in Fig. 1 have been checked by changes in  $\Delta$  values. 2-Vinylpyridine (I) has been chosen as a model compound.  $T_1^i(i)$ ,  $T_1^i(ij)$ , and  $T_1^i(\text{all})$  for all protons of I were measured.

$$f_{ij} = \frac{R^i(ij) - R^i(i)}{R^i(\text{all}) - R^i(i)} \quad (1)$$

$$f_{ij} = \frac{N_j \sigma_{ij}}{\sum_j N_j \sigma_{ij}} = \frac{N_j \rho_{ij}}{\sum_j N_j \rho_{ij}} \quad (2)$$

so  $f_{i1} : f_{i2} : \dots : f_{ij} = r_{i1}^{-6} : r_{i2}^{-6} : \dots : r_{ij}^{-6}$  (3)  
 $f_{ij}$  values obtained from equation (1) should be correlated with H-H distances ( $r_{ij}$ ) as shown in equation (3), assuming molecular isotropic motion. For one possible conformation, every H-H distance from the Dreiding model and the three measured sets of  $T_1$  data are used as input, and the calculation to check the best giving the correlation coefficient (R). For I, the calculations have been carried out for three possible conformations (A, B, and C) and the correlation coefficients have been compared. Conformation A has the largest coefficient suggesting the optimum conformation.

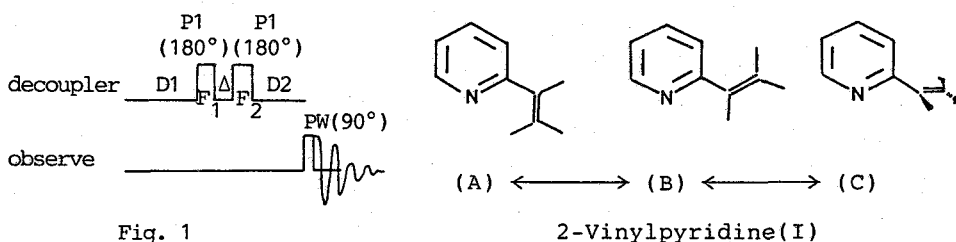


Fig. 1

MOLECULAR DYNAMICS AND CHEMICAL STRUCTURE OF STREPTOMYCIN  
IN SOLUTION DETERMINED FROM RELAXATION TIME ANALYSIS

Masayuki Watanabe, Hideaki Fujiwara, Tatsuya Takagi  
and Yoshio Sasaki

Faculty of Pharmaceutical Sciences, Osaka University,  
Suita, Osaka

Makiko Sugiura

Kobe Women's College of Pharmacy, Higashinada-ku, Kobe

NMR relaxation data provide information related to molecular dynamics and structure in solution. A simplest model for the molecular motion is "isotropic model", which is used extensively in routine works. But for nonsymmetrical molecules the overall motion is expected to be anisotropic, and additional correlation times (or inversely related diffusion coefficients) are required to describe differential rates about molecular diffusion axes. We have examined antibiotics streptomycin sulphate by means of an isotropic model based on the  $^{13}\text{C}$  and  $^1\text{H}$   $T_1$  data.

$T_1$  measurements were made using inversion-recovery method at 200MHz for  $^1\text{H}$  and at 22.6MHz for  $^{13}\text{C}$ . Concentrations of the samples were 0.07M ( $^1\text{H}$ ) and 0.44M ( $^{13}\text{C}$ ). Also  $^{13}\text{C}$  and  $^1\text{H}$  resonances in streptomycin were assigned with the aid of COSY and decoupling techniques. First, we assumed the isotropic model for the interpretation of the  $T_1$  data, which led to the diffusion constant of  $1.2 \times 10^7 \text{ sec}^{-1}$  for  $^1\text{H}$  in contrast with  $2.4 \times 10^5 \text{ sec}^{-1}$  for  $^{13}\text{C}$ . Secondly, "symmetric top model" was assumed. This has given two diffusion constants of  $D_1 = 9.8 \times 10^8 \text{ sec}^{-1}$  and  $D_2 = 2.0 \times 10^8 \text{ sec}^{-1}$  from  $^1\text{H}$  data in a rather excellent agreement with those of  $D_1 = 14.6 \times 10^8 \text{ sec}^{-1}$  and  $D_2 = 3.5 \times 10^8 \text{ sec}^{-1}$  from  $^{13}\text{C}$  data. As regards the structure, an extraordinary short C-H distance was found in the published X-ray data, whereas the corresponding  $^{13}\text{C}$   $T_1$  value was observed in the normal range.

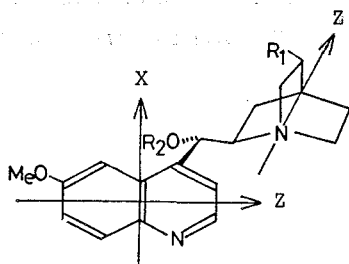
# $^{13}\text{C}$ Studies of the Anisotropic Motion of Quinidine Derivatives

Torei Sai, Makiko Sugiura, and Narao Takao

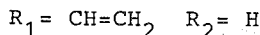
Kobe Women's College of Pharmacy, Higashinada-ku, Kobe, Japan

$^{13}\text{C}$  measurements are very important since they provide detailed information concerning molecular stereochemistry and molecular motion in solution. In the present study, this technique was applied to the study of molecular motions of quinidine, which is commonly used as an antiarrhythmia drug, and its derivatives.

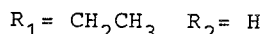
Quinidine(1), dihydroquinidine(2), and acetylquinidine(3) have been studied. Quinoline and quinuclidine have been used as reference compounds.  $^{13}\text{C}$  and N.O.E. measurements were obtained in  $\text{CDCl}_3$  (0.3 mol/l) solution. We have calculated anisotropic motion using  $T_1^{\text{DD}}$ . Diffusion rates around the long axis ( $D_1$ ) and the short axis ( $D_2$ ), which is perpendicular to the long axis were obtained, together with geometric factors ( $\theta, \phi$ ) which show the direction of the long axis for which  $[1/T_1^{\text{DD}}(\text{obsd.}) - 1/T_1^{\text{DD}}(\text{calcd.})]^2$  is minimized. We separate quinidine into the quinoline part and the quinuclidine one. The diffusion rates for 3 are much bigger than those of 1 and 2. This result shows that 1 and 2 seem to exist as a dimer in  $\text{CDCl}_3$  because of hydrogen bonding of the hydroxy group, while 3 is present in solution as a monomer. The diffusion rates for 2 are also a bit smaller than those for 1 as the size of molecule becomes bigger by reduction. The diffusion rates for the quinuclidine part are bigger compared with the quinoline part. For the quinoline part, quinidine derivatives rotate predominantly around the X axis while quinoline rotates predominantly around the Z axis. A deviation of the main axis from the X axis is observed with derivatives with different substituent groups and different species (monomer or dimer) in  $\text{CDCl}_3$ . For the quinuclidine part, both quinidine derivatives and quinuclidine rotate predominantly around the Z axis. But the main axis also deviates from the Z axis, and this also varies with the derivatives.



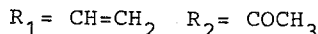
Quinidine (1)



Dihydroquinidine (2)



Acetylquinidine (3)



LOCATIONS OF LOCAL ANESTHETICS AND THEIR DYNAMICAL PERTURBATIONS  
FOR LIPIDS IN PHOSPHATIDYLCHOLINE VESICLES AS STUDIED BY NUCLEAR  
OVERHAUSER EFFECTS IN  $^1\text{H}$  NUCLEAR MAGNETIC RESONANCE SPECTROSCOPY

Yoshihiro Kuroda and Yasuhiro Fujiwara

Faculty of Pharmaceutical Sciences, Kyoto University, Sakyo-ku,  
Kyoto, Japan and Kyoto Pharmaceutical University, Yamashina-ku,  
Kyoto, Japan

Locations and dynamical perturbations for lipids of local anesthetics (procaine.HCl, tetracaine.HCl, and dibucaine.HCl) in sonicated egg yolk phosphatidylcholine (PC) vesicles have been studied by  $^1\text{H}$ - $^1\text{H}$  nuclear Overhauser effect (NOE) measurements. It was found that tetracaine and dibucaine bind much strongly to the neutral lipids than procaine does and that their mobilities are lowered to such an extent that transmits spin diffusion (i.e.,  $\omega^2\tau_c^2 \gg 1$ ). The intermolecular NOEs between drugs and PC were more effective in dibucaine than in tetracaine, indicating that dibucaine binds to the lipids more strongly than tetracaine; this order agrees well with that of anesthetic potency. However, it was only the tetracaine that showed an appreciable extent of dynamical perturbations to the PC vesicles, when they were monitored by the extent of transfer of the negative NOE from  $\alpha$ -methylene protons to choline methyls, olefinic methines, acyl methylenes and terminal methyl protons. This finding was interpreted as being due to the differences in the locations of these drugs in small unilamellar vesicles: (1) procaine interacts with lipids very weakly at the outer surface of the vesicles; (2) tetracaine binds to the lipids both at the outer and inner halves of the bilayer inserting its rod-like molecule in a forest of acyl chains of PC; (3) dibucaine binds tightly to the polar head group of PC which resides only at the outer half of the bilayer vesicles. It was concluded that the relative order of anesthetic potency within these drugs can be correlated not with the ability to affect membrane fluidity but with the ability that binds to lipids at the polar head group of the bilayer vesicles.

A NEW NOE TECHNIQUE USING HIGHLY SELECTIVE IRRADIATION FREQUENCY  
USEFUL FOR STRUCTURAL STUDIES OF NATURAL PRODUCTS

Kazuo Furihata, Haruo Seto and Muneki Ohuchi\*

Institute of Applied Microbiology, The University of Tokyo,  
Bunkyo-ku, Tokyo, \*JEOL CO., Nakagami, Akishima, Tokyo, Japan

In the structural studies of complicated natural products, nuclear Overhauser effect (NOE) gives very important information to connect proton spin systems separated by a quaternary or heteroatom and to analyze stereochemical relationships. One problem associated with NOE experiment, however, is the occurrence of selective population transfer (SPT) in the strongly coupled spin systems, which causes the analysis of NOE very difficult.

So far reported, the composite pulse technique reported by Bauer is an excellent method which enables to overcome this problem. We have modified his method by replacing Gaussian pulse with time sharing decoupling (DANTE). This modified method gives very excellent results with regard to high selectivity and easier operation.

In addition, application of this method to the new NOE experiments in the rotating frame (ROESY) gave excellent results.



APPLICATION OF HETERONUCLEAR DOUBLE QUANTUM COHERENCE NMR FOR  
STRUCTURAL STUDIES OF NATURAL PRODUCTS

Muneki Ohuchi, Nobuaki Yokoyama, Yutaka Fukushima,  
Kazuo Furihata\* and Haruo Seto\*

JEOL CO., Nakagami, Akishima, Tokyo, \*Institute of Applied  
Microbiology, University of Tokyo, Bunkyo-ku, Tokyo, Japan

Several techniques have recently been introduced to improve the low sensitivity of NMR spectroscopy. Among them, the most interesting and important methods would be those proposed by Bax et al., i.e., HMQC and HMBC, which reveal the shift correlation between the proton and heteronucleus by observing the most sensitive  $^1\text{H}$  nucleus. Their application to complicated natural products, however, has not been investigated in detail.

After many experimental investigations, we have established the most suitable experimental conditions necessary for these techniques, and attempted their application to the structural analysis of a new polyether antibiotic portmicin. As a result, these methods turned out to be extremely powerful methods for structural studies of complicated molecules. However, even these new techniques suffer from a disadvantage of 2D NMR being very time-consuming. In order to overcome this problem, we have attempted to modify these technique by decreasing the column points in order to make partial observation of these 2D NMR spectra and have obtained satisfactory results. In this paper, application of this 2D NMR and its partial observation to natural products will be reported.

Structures of New Triterpenoids from Chinese Crude Drug  
"Ban Zhi Lian" (*Scutellaria rivularis*) ----- Application  
of 2-D INADEQUATE and Long-Range  $^1\text{H}$ - $^{13}\text{C}$  COSY

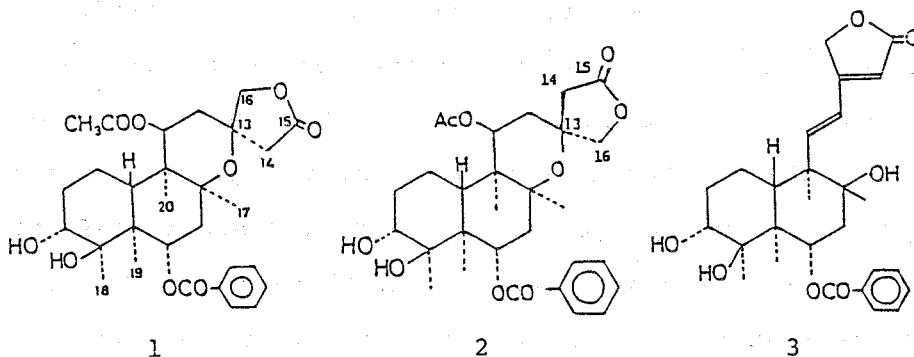
Tohru Kikuchi,<sup>a)</sup> Shigetoshi Kadota,<sup>a)</sup> Koji Tsubono,<sup>a)</sup>  
Tsuyoshi Tomimori,<sup>b)</sup> Haruhisa Kizu,<sup>b)</sup> and  
Yoshitake Imoto<sup>b)</sup>

Research Institute for Wakan-Yaku (Oriental Medicines),  
Toyama Medical and Pharmaceutical University,<sup>a)</sup> Toyama,  
Japan and School of Pharmacy, Hokuriku University,<sup>b)</sup>  
Kanazawa, Japan

Diterpene Components of Chinese crude drug "Ban Zhi Lian"  
(*Scutellaria rivularis*) were examined.

The ether soluble fraction obtained from the ethanol extract  
was separated by silica gel chromatography followed by prepara-  
tive HPLC to give new diterpenoids, designated as scuterivu-  
lactone C1(1), C2(2) (isolated as acetate), and D(3), along with  
fourteen flavonoids. The structures of these diterpenoids were  
determined by means of the two-dimensional (2-D) NMR including  
2-D INADEQUATE (Incredible Natural Abundance Double Quantum  
Transfer Experiment) and long-range  $^1\text{H}$ - $^{13}\text{C}$  COSY. The stereo-  
chemistry was assigned on the basis of the coupling constants  
and the NOE experiments.

Also the  $^{13}\text{C}$ -NMR spectra were analysed in detail and the  
assignments of their carbon signals were done on the basis of  
DEPT and 2D-NMR methods.



<sup>13</sup>C AND <sup>31</sup>P NMR STUDY OF ORGANIC ANIONS PRODUCED FROM PHENYL  
AND DIPHENYLPHOSPHINES

Yukihiro Yokoyama and Kensuke Takahashi

Department of Applied Chemistry, Nagoya Institute of  
Technology, Gokiso-cho, Showa-ku, Nagoya 466

We report here the <sup>13</sup>C and <sup>31</sup>P NMR parameters of PhPHLi and Ph<sub>2</sub>PM (M=Li, Na, K) in several solvents. The effects of solvents and counter cations on the <sup>13</sup>C and <sup>31</sup>P chemical shifts and coupling constants are discussed.

In the compounds studied anionization results in large <sup>13</sup>C shifts to lower field for the ipso carbon atoms and to upper field for the para carbon atoms as shown in Table 1. It is found that the changes of shifts of the ipso and para carbons in the anions produced from phenylphosphines are larger than those in anilidelithium. It seems that the degree of delocalization of the anions is larger than that of anilidelithium.

When phenylphosphines are anionized, <sup>31</sup>P NMR signals shift to lower field, while the one-bond <sup>31</sup>P-<sup>13</sup>C coupling constants extremely increase in magnitude. It seems that the changes of the NMR parameters are affected by not only excess charge, but also hybridization, as well as in the case of anilidelithium.

It is of interest to note that solvent and counter cation play a significant role in the <sup>13</sup>C and <sup>31</sup>P chemical shifts, and <sup>31</sup>P-<sup>13</sup>C and <sup>31</sup>P-<sup>1</sup>H coupling constants of these anions. The NMR parameter changes are larger in solvents with stronger polarity. Therefore, it seems that the large changes of chemical shifts and coupling constants are due to the structure of ion-pairing in the anion solutions.

Table 1. The chemical shifts (ppm)<sup>a</sup> and coupling constants (Hz) of phenylphosphine and its lithium salt in several solvents

Compd/Solv.	$\delta C_i$	$\delta C_o$	$\delta C_m$	$\delta C_p$	$\delta P$	$^1J_{PC}$	$^1J_{PH}$
PhPH <sub>2</sub> /THF	129.21	135.33	129.15	128.79	-125.4	10	199
PhPHLi/THF	161.63	129.91	126.80	116.53	-112.6	43	163
/DME	160.95	129.96	126.77	116.72	-111.9	44	163
/2MTHF	158.05	130.27	126.57	117.70	-114.3	37	172
/HMPA	170.27	127.80	125.46	110.54	-74.9	59	144

a) Referred to TMS for <sup>13</sup>C and H<sub>3</sub>PO<sub>4</sub> for <sup>31</sup>P.

THE ORIGIN OF SOLVENT EFFECT ON THE CHEMICAL SHIFT OF METAL  
NUCLEAR MAGNETIC RESONANCE

Megumu Munakata, Susumu Kitagawa and Manabu Sasaki

Department of Chemistry, Faculty of Science and Technology,  
Kinki University, Kowakae, Higasi-Osaka 577, Japan

The metal NMR resonance of a metal ion is remarkably sensitive to the solvent.  $^{23}\text{Na}$  shifts have been reported to correlate well with donor numbers for ten solvents. But water and methanol deviate from the correlation. Such correlation is not satisfactory for  $^7\text{Li}$ ,  $^{39}\text{K}$  and  $^{133}\text{Cs}$  shifts.

$^{65}\text{Zn}$ ,  $^{113}\text{Cd}$  and  $^{205}\text{Tl}$  shifts in donor solvents correlate neither with donor number nor fundamental properties of the solvents such as dielectric constant and Z value. Thus, one has been so far forced to conclude that there are no wide-ranging correlations between metal chemical shifts and solvent properties. This should be attributable to the absence of a good measure for donor ability of a solvent. We have been proposed coordination power (CP) as a measure for the donor ability which is related to Gibbs free energy change on the solvation of nickel(II) ions (Inorg. Chem. 1985, 24, 1638).

$$\text{CP} = 1/6 \log([\text{NiS}_6][\text{MeCN}]^6 / [\text{Ni}(\text{MeCN})_6][\text{S}]^6), \text{ S=solvent}$$

$^{113}\text{Cd}$  NMR resonances of 1 M  $\text{Cd}^{2+}$  ion in alcohol and nitrile series were measured and were found to shift downfield with increasing CP of the alcohol and nitrile, respectively.  $^{108}\text{Ag}$  shifts were obtained for 1 M  $\text{AgClO}_4$  solution. It was also found that  $^{108}\text{Ag}$  shifts in nitrile correlate well with CP of the nitrile: The deshielding of  $^{108}\text{Ag}$  nucleus increases with increasing of CP. The remarkable downfield shifts were obtained because of the specific interaction between  $\text{Ag}^+$  and nitrile. Such good correlation was not obtained for alcohol and ketone series, respectively. This suggests that the coordination number of silver (I) solvate ions is not always the same in the latter two solvent series.

# CALCULATION OF NMR CHEMICAL SHIFTS

## BY A GAUGE-INVARIANT INDO METHOD

Hiroyuki Fukui, Koichi Miura, and Akihiko Hirai

Kitami Institute of Technology

165 Koencho, Kitami, Hokkaido 090, Japan

A gauge-invariant INDO method based on the coupled Hartree-Fock perturbation theory is presented and applied to the calculation of  $^1\text{H}$  and  $^{13}\text{C}$  chemical shifts of hydrocarbons including ring compounds. Invariance of the diamagnetic and paramagnetic shieldings with respect to displacement of the coordinate origin is discussed. Comparison between calculated and experimental results exhibits fairly good agreement, provided that the INDO parameters of Ellis *et al.* (*J. Am. Chem. Soc.* 94, 4069 (1972)) are used with the inclusion of all multicenter one-electron integrals.

EFFECT OF RARE SPIN  $^{17}\text{O}$  ON THE SPIN-LATTICE RELAXATION TIME  
 $T_{1\rho}$  OF PROTONS IN THE ROTATING FRAME: STUDY IN SOME SULFATES

Kunihiko MORIMOTO

Faculty of the Integrated Arts and Sciences, Hiroshima

University, Hiroshima 730, Japan

Recently we found the rare spin  $^{17}\text{O}$  (0.037% natural abundance) has a pronounced effect on the spin-lattice relaxation time  $T_{1\rho}$  of protons ( $^1\text{H}$ ) in the rotating frame in some solids.<sup>1)</sup> In the present study the temperature dependence of  $T_{1\rho}$  of  $^1\text{H}$  was measured in some sulfates<sup>2)</sup>  $(\text{NH}_4)_2\text{S}_2\text{O}_8$ ,  $\text{NH}_4\text{HSO}_4$  and  $\text{KHSO}_4$  in order to investigate the rotational diffusion (reorientation) of the oxygen atoms in  $\text{SO}_4$  group. It was found that three large minima (1-3sec) should appear in the temperature dependence of  $T_{1\rho}$  of  $^1\text{H}$  in general; one minimum due to (A) modulation of the dipolar interaction between the  $^1\text{H}$  and  $^{17}\text{O}$  spins by the reorientation of  $\text{SO}_4$  group and two minima due to (B) cross relaxation between the  $^1\text{H}$  and  $^{17}\text{O}$  spins as

$$T_{1\rho}^{-1} = A_1 f_L(\omega_1, \tau_a) + A_2 f_L(\omega_1, T_{1S}) \quad (1)$$

$$T_{1S}^{-1} = 8/1875 (e^2 q Q / \hbar)^2 \left\{ f_L(\omega_S, \tau_a) + 4 f_L(2\omega_S, \tau_a) \right\} \quad (2)$$

where  $\omega_1 = \gamma \text{H}_1$  is the Larmor frequency of  $^1\text{H}$  in the rotating frame,  $\tau_a$  the correlation time of the reorientation of  $\text{SO}_4$  group,  $T_{1S}$  the spin-lattice relaxation time of  $^{17}\text{O}$  spin,  $e^2 q Q / \hbar$  the quadrupole coupling constant of  $^{17}\text{O}$  and  $f_L(\omega, \tau) = \tau / (1 + \omega^2 \tau^2)$ . The temperature dependence of  $T_{1\rho}$  in three sulfates shows large minima (1-3sec) due to the interaction between the  $^1\text{H}$  and  $^{17}\text{O}$  spins. The values  $\tau_a$ ,  $T_{1S}$  and  $e^2 q Q / \hbar$  of  $^{17}\text{O}$  were determined by using Eqs. (1) and (2). In some compounds in which  $T_1$  of  $^1\text{H}$  is larger than a few seconds, the measurement of  $T_{1\rho}$  might make possible to determine  $T_{1S}$  and  $e^2 q Q / \hbar$  of  $^{17}\text{O}$ . 1) K. Morimoto and K. Shimomura; J. Phys. Soc. Jpn. 53 (1984) 2752, J. Phys. C 18 (1985) 403, J. Phys. Soc. Jpn. 54 (1985) 3244, Phys. Lett. A 116 (1986) 85. 2) T. Chiba and S. Miyajima; J. Chem. Phys. 83 (1985) 6385.

NUCLEAR MAGNETIC RESONANCE STUDIES OF PROTONATION AND MERCURIATION  
OF TRIPHENYLPHOSPHONIUM CYCLOPENTADIENILIDE

Chikakiyo Nagata and Kaoru Yamada

Department of Industrial Chemistry, Shibaura Institute of  
Technology, Minato-ku, Tokyo, Japan

In order to elucidate the structure of the reaction products between triphenylphosphonium cyclopentadienilide ( $\text{ph}_3\text{PCp}$ ) and trifluoroacetic acid and mercuric halide ( $\text{HgX}_2$ ;  $\text{X}=\text{Cl}, \text{Br}$ ), respectively, we measured  $^1\text{H}$ ,  $^{13}\text{C}$  and  $^{199}\text{Hg}$  NMR spectra.

The  $^{13}\text{C}$  signals of the cyclopentadienyl (Cp) ring of  $\text{ph}_3\text{PCp}$  in  $\text{CF}_3\text{CO}_2\text{H}$  solution appeared at 46.4, 125.3, 134.4, 148.5 and 158.7 ppm (from TMS), and these peaks are splitted to doublet by the spin coupling with  $^{31}\text{P}$ . By the consideration of the amplitudes of the coupling constants ( $J_{\text{cp}}$ ) with  $^{31}\text{P}$  and also of the  $^{13}\text{C}$  chemical shifts of  $\text{ph}_3\text{PCp}$ , the site of protonation was determined as the 3-position of the Cp ring.

The site of interaction between the Hg atom and Cp ring in complexes of  $\text{CpHgX}_2$  ( $\text{X}=\text{Cl}, \text{Br}$ ) has been a subject of debate for long time. By means of X-ray diffraction method, Holy et al. determined the site of attachment of the Hg atom as the C-3 position. However, from the  $^{13}\text{C}$  NMR spectra of the mercury complexes in DMSO, they proposed that the nature of the Hg-Cp interaction in solution is fluxional  $\sigma$ -bonding. Our  $^{13}\text{C}$  NMR data supported this proposition. Further confirmation of the fluxional  $\sigma$ -bonding was obtained by the measurement of the  $^{199}\text{Hg}$  NMR spectra of  $\text{ph}_3\text{PCp}\cdot\text{HgCl}_2$  complex in  $\text{DMSO-d}_6$  solution, where the  $^{199}\text{Hg}$  signal appeared at 273 ppm (from  $\text{HgCl}_2$ ). These results indicate that the protonation occurs predominantly at the C-3 position of the Cp ring, whereas the mercury is not attached at a definite site but is interacted via fluxional  $\sigma$ -bonding.

ASSIGNMENT OF THE  $^{13}\text{C}$  NMR RESONANCES OF POLY(OLEFINE)S TO THE TACTICITY ON THE BASIS OF THE CHEMICAL SHIFT CALCULATION

Tetsuo Asakura and Yuko Nishiyama

Department of Polymer Engineering, Faculty of Technology,  
Tokyo University of Agriculture and Technology,  
Koganei, Tokyo, Japan.

It is possible to use theoretical chemical shift calculations on the basis of  $^{13}\text{C}$  NMR  $\gamma$  effect to the chemical shift and the application of the rotational isomeric state, r.i.s. model to the polymer conformation as a reliable method of the peak assignment due to the polymer tacticity. Moreover, if the agreement between the calculated and observed chemical shift was obtained, we can analyze rigorously the time-averaged polymer conformation in solution from the bond probabilities obtained with the r.i.s. model at the same time.

In this study,  $^{13}\text{C}$  NMR chemical shift of regioirregular polypropylene, PP, is calculated on the basis of  $^{13}\text{C}$  NMR chemical shift  $\gamma$  effect and application of the r.i.s. model to the local conformation of the inverted PP portions. In addition, in order to obtain the  $^{13}\text{C}$  chemical shifts of regioirregular PP, the  $^{13}\text{C}$  NMR spectra of regioirregular syndiotactic and atactic PP samples are observed. Especially, the INEPT spectra are obtained to identify small peaks of the carbons located at the inverted portion to the methine, methylene and methyl carbons and also, to distinguish the methine carbon peaks from the methylene ones when these peaks overlapped. In the tail-to-tail sequence, the spectra of the  $T_{\beta\gamma}$  carbon which is observed as a singlet peak and the  $S_{\gamma\alpha\beta\delta}$  carbon which is splitted roughly into two peaks with peak separation of about 1 ppm are well reproduced. The splitting into two peaks is also predicted for the  $P_{\beta\gamma}$  carbon although the peak is not observed because of the presence of main methyl peaks of the head-to-tail sequence. Similarly, the spectral character of  $T_{\alpha\beta}$ ,  $S_{\beta\alpha\alpha\gamma}$  and  $P_{\alpha\beta}$  carbons in the head-to-head sequence are also well reproduced.

In conclusion, these theoretical chemical shift calculation on the basis of  $^{13}\text{C}$  NMR  $\gamma$  effect and application of the r.i.s. model is very useful for the purpose of assignment of the regioirregular PP spectrum to the tacticity as well as stereoirregular PP, poly(1-butene) and ethylene-propylene copolymer.



**<sup>15</sup>N- and <sup>17</sup>O-NMR Substituent Chemical Shifts of Pyridine 1-Oxides:  
A Multiple Multinuclear Approach to the Dual Resonance Effects**

Masami Sawada, Yoshio Takai, Satoshi Kimura, Satoshi Yamano,  
Soichi Misumi, Yuho Tsuno, Terukiyo Hanafusa

Material Analysis Center, the Institute of Scientific and  
Industrial Research, Osaka University, Suita, Osaka 567

Pyridine 1-oxide is an interesting system for us to study electronic substituent effects on reactivities and/or physical properties because of the very unique N-O functionality which can act effectively in both directions as a pi-electron donor and a pi-electron acceptor function. However, there are very few where this historically accepted dual N-oxide functionality has been apparently expressed by means of a quantitatively treated equation on the basis of a systematic change of both 3- and 4-substituents.

<sup>15</sup>N- and <sup>17</sup>O-NMR spectra of the same series of substituted pyridine 1-oxides were measured at natural abundance in DMSO, and their resulting sets of substituent chemical shifts(SCSs) were correlated with those of several related systems, and tested whether this type of dual functionality really exists or not in the pyridine 1-oxide system.

(1) <sup>17</sup>O SCSs of the 4-substituents show clearly the dual resonance contributions of the unique N-oxide system and include enough the inductive contribution.

(2) <sup>17</sup>O SCSs of the 3-substituents correlate better with  $\sigma_I$  scale just like the <sup>19</sup>F SCSs of meta-substituted fluorobenzenes and the quantities of ( $\Delta\delta^{17}O_4 - \Delta\delta^{17}O_3$ ) give a bilinear relationship with the resonance scale of  $\sigma_\pi^+$  and  $\sigma_\pi^-$ .

(3) <sup>15</sup>N SCSs of the 4- (and 3-) substituents bilinearly correlate with the corresponding <sup>13</sup>C SCSs of mono-substituted benzenes, indicating they are mainly controlled by resonance effect and negligible inductive one.

(4) In spite of completely different contributions of the inductive effects on <sup>17</sup>O and <sup>15</sup>N, the resonance susceptibility ratios,  $\rho_\pi^+/\rho_\pi^-$  values, keep constant between <sup>17</sup>O and <sup>15</sup>N in the pyridine 1-oxide system.

$$SCS = \rho_i \sigma_i + \rho_\pi^+ \sigma_\pi^+ + \rho_\pi^- \sigma_\pi^-$$

Functions and Characteristics of the NMR Section in the Supermini-Computer System of Material Analysis Center (TASMAC) :

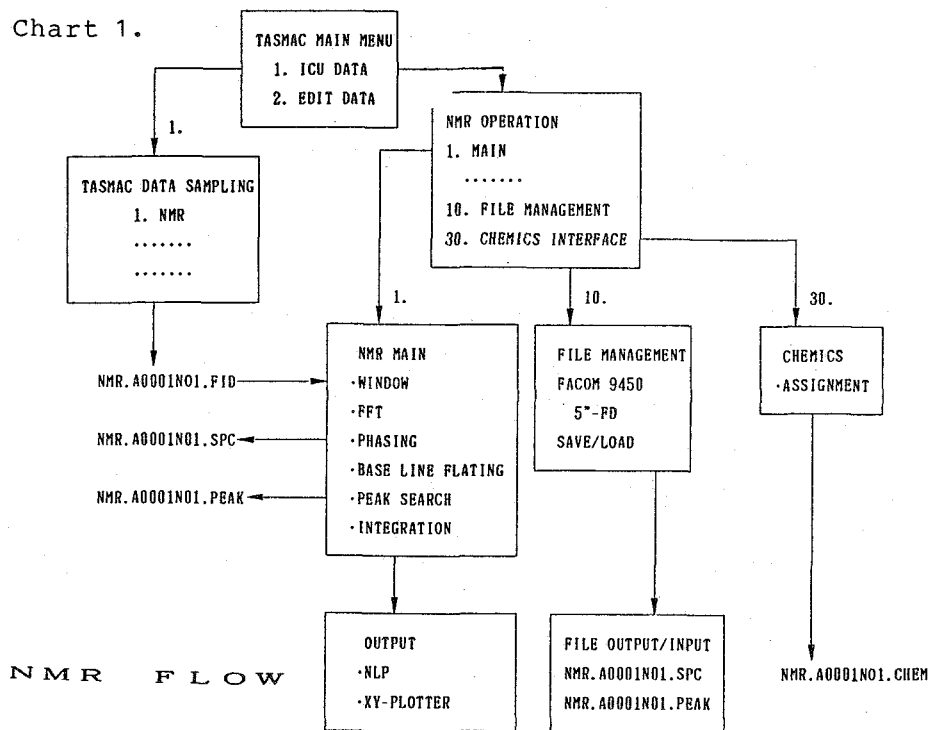
FID Data Receive, Processing, and Linkage to CHEMICS

Yoshio Takai, Hitoshi Yamada, Fusako Fukuda, Takanori Tanaka, Masami Sawada, Terukiyo Hanafusa

Material Analysis Center, the Institute of Scientific and Industrial Research, Osaka University, Suita, Osaka 567

Material Analysis Center (MAC), ISIR, Osaka Univ. has developed a supermini-computer system called TASMAC which can process data from a variety of analytical instruments such as NMR, MS, IR, UV etc. The TASMAC is intended to a system of their total analysis.

Here, we describe a computer program of the NMR section. It is mainly constructed by three modules, that is, (1) NMR data receiving from ASPECT3000, Bruker AM360, to FACOM S3500, Fujitsu, via RS232C, (2) NMR data processing, and (3) linkage to CHEMICS/version 6 (a computer-assisted structure elucidation system of organic compounds: a program constructed by prof. Shin-ichi Sasaki). When a user follows the next processes (Chart 1), he can know all possible structures of the organic molecule in the output of NLP. The outline of our "menu" flow is in Chart 1.



NMR Studies of Behavior of Molecules in Polymer Films (III);  
Comparison between Cellulose-Triacetate and Cellulose Films  
Kazunori Matsumura, Kikuko Hayamizu, Takashi Nakane,  
Hiroshi Yanagishita and Osamu Yamamoto  
National Chemical Laboratory for Industry,  
Tsukuba Research Center, Ibaraki 305, Japan

At the 24th NMR Conference and the 52th Annual Meeting of the Chemical Society of Japan, we presented the  $^1\text{H}$  and  $^2\text{H}$  NMR studies of water and methanol contained in the cellulose acetate (CA) film. The employed CA includes approximately 2.5 acetyl groups and 0.5 hydroxyl groups per one pyranose ring on an average. Therefore in the CA film water or methanol are probably bonded both to acetyl C=O and hydroxyl O-H, which makes it complicated to interpret the behavior of these molecules in the film. This time using the cellulose triacetate (CTA) film which has 3 acetyl groups and the cellulose (CEL) film which has 3 hydroxyl groups, we present the studies of  $^1\text{H}$  and  $^2\text{H}$  NMR spectra of  $\text{H}_2\text{O}$  and  $\text{D}_2\text{O}$  in these films.

NMR spectra are observed changing the angle between the surface of the film and the magnetic field to determine the orientation of water molecules in these films. It is found that water molecules in the CTA film have a tendency to orient perpendicularly to the surface of the film, while in the CEL film to orient parallel. The line width of water in the CEL film is broader than that in the CTA film, which suggests that the water molecules are bonded to the CEL film more tightly than to the CTA film. The temperature dependences of spectra are also observed to determine the mobility of the water molecules in these films. Comparing between  $^1\text{H}$  and  $^2\text{H}$  NMR spectra, we obtained the information about the proton exchange between the different water molecules or between the water molecules and the film materials.

USE OF THE NUCLEAR OVERHAUSER EFFECT FOR STRUCTURE-ANALYSIS  
STUDIES OF AROMATIC POLYAMIDEIMIDES AND RELATED COMPOUNDS

Katsuyuki Yokota

Toray Research Center, Inc., Ohe-cho, Minato-ku, Nagoya, Japan

The proton-proton nuclear Overhauser effect (NOE) has been used for structure-analysis studies of aromatic polyamideimides and related compounds. Experiments were performed with oligoamide prepared from m-phenylenediamine and isophthalic acid (oligo-(mP/IPA)), polyamideimide from 4,4'-diaminodiphenylether and trimellitic acid (poly(DDE/TMA)), and other polymers. The results obtained demonstrate that the NOE or spin-diffusion experiments are useful to obtain both resonance assignments and information of monomer sequence in such oligomer and polymer systems.

Most of the resonances in the  $^1\text{H}$  spectrum of oligo(mP/IPA) are assigned based on both the COSY experiments and chemical shifts. These assignments show that by irradiation of the amide protons, NOEs are produced on the protons of the adjacent acid residues as well as the amine residues. The resonances could therefore be sequentially assigned by the combined use of COSY and NOE without consideration of the chemical shifts. Application of a similar procedure to the polymer systems is also suggested.

It is found that the NOEs observed on poly(DDE/TMA) and other polymers are not completely non-specific, although they are greatly influenced by spin diffusion. On the basis of both the J-coupling and spin-diffusion networks obtained, the  $^1\text{H}$  spectrum of poly(DDE/TMA) can be assigned to the three possible structures, i.e., head to tail, head to head, and tail to tail structures. These results indicate that spin diffusion across the ether bond or imide bond is effectively suppressed, which is probably the main reason that makes the NOE experiments useful in these systems. The author thus suggests that the NOE or spin-diffusion experiments could be generally applied to obtain information of local structure or particular components in the polymer mixture systems where some spin-diffusion barrier is present.

MULTIPLE QUANTUM 2D-NMR:  
APPLICATION TO STRUCTURAL ANALYSIS OF POLYMERS

Mitsuhiko Ikura, Manabu Yasuda, Tohru Katoh, Kunio Hikichi,  
Muneki Ohuchi\*, and Keiji Eguchi\*  
High-Resolution NMR Laboratory and Department of Polymer Science,  
Faculty of Science, Hokkaido University, Sapporo, and \*JEOL Co.  
Ltd., Tokyo, Japan

The multiple quantum spectroscopy has been extensively used for the study of structure of ordered phase. For isotropic solution, double quantum spectroscopy has been mainly utilized for analyzing  $^1\text{H}$  and  $^{13}\text{C}$  spectra of complex organic compounds. The purpose of this paper is to examine utility of the multiple quantum 2D-NMR spectroscopy for analyzing structure of synthetic polymers including atactic poly(vinyl alcohol) (PVA), poly(propylene oxide) (PPO), and polybutadiene (PB).

Experimental: PVA was dissolved in  $\text{D}_2\text{O}$  at a concentration of 10wt%. PPO was dissolved in  $\text{C}_6\text{D}_6$  at a concentration of ca. 80wt%. PB was dissolved in  $\text{CDCl}_2\text{CDCl}_2$  at a concentration of 19wt%. 2D-NMR spectra were observed using JEOL GX-500 and GX-400 spectrometers equipped with a phase shifter of  $22.5^\circ$ ,  $30^\circ$ ,  $45^\circ$ , and  $60^\circ$  in addition to  $0^\circ$ ,  $90^\circ$ ,  $180^\circ$ , and  $270^\circ$  phases. Experimental methods of 2D-NMR were described elsewhere.

Results and Discussion:  $^1\text{H}$ - $^1\text{H}$  double quantum coherence echo correlated spectroscopy (DECSY) was applied to analyze configuration of PVA. DECSY provides an important information about chemically equivalent protons of  $\text{CH}_2$  in rrr and mrm tetrad sequences. Triple quantum filtered COSY with broad-band decoupling of  $F_1$  axis can be utilized for selective detection of nonequivalent resonances of  $\text{CH}_2$  group of PVA.  $^{13}\text{C}$ - $^{13}\text{C}$  DECSY is preferable to INADEQUATE for the analysis of connectivities between CH and  $\text{CH}_2$  carbons of PPO, because the  $F_1$  spectral width of DECSY is 2 times narrower than that of INADEQUATE.  $^{13}\text{C}$ - $^{13}\text{C}$  DECSY was also applied to PB and we found that two large  $\text{CH}_2$  peaks of 1,4-trans and 1,4-cis stereoisomers were connected each other through  $^{13}\text{C}$ - $^{13}\text{C}$  coupling. Therefore, the PB sample used here is a random copolymer.

GAS-PHASE  $^{19}\text{F}$  AND  $^1\text{H}$  HIGH-RESOLUTION NMR SPECTROSCOPY:  
APPLICATION TO THE STUDY OF UNPERTURBED CONFORMATIONAL ENERGIES  
OF 1,2-DIFLUOROETHANE

Shinji Nonoyama, Takashi Miyajima, Tokiji Kawamura,  
and Tsuneo Hirano

Department of Synthetic Chemistry, Faculty of Engineering,  
University of Tokyo, 7-3-1 Hongo, Bunkyo-ku, Tokyo 113, Japan

We studied the conformational equilibrium of 1,2-difluoroethane through the gas-phase  $^{19}\text{F}$  and  $^1\text{H}$  NMR coupling constants, hoping to obtain conformational energies and to settle the longstanding debate on the experimental values reported in a wide range (0 to -1.76 kcal/mol).

Gas-phase NMR spectra were observed at eight temperatures on a JEOL GX-400 for  $^{19}\text{F}$  at 376 MHz, and for  $^1\text{H}$  at 400 MHz. Chemical shifts are given in p.p.m. downfield from the gaseous internal standards  $\text{CFCl}_3$  for  $^{19}\text{F}$  and TMS for  $^1\text{H}$ .

The  $^{19}\text{F}$  and  $^1\text{H}$  NMR spectra as sets were analyzed as the AA'A"XX' spin system with the aid of LAOCN3 program. Under the rotational isomeric state model and the assumption of Boltzman distribution, the conformational energy difference between the gauche and trans states has been estimated from the coupling constants observed in the  $^{19}\text{F}$  and  $^1\text{H}$  NMR spectra.

Values relative to Trans-state	Our values (Uncert. Sigma)	Abraham's value <sup>a)</sup>
$\Delta G$ in kcal/mol	-0.85 (0.16)	0.60
$\Delta H$ in kcal/mol	-1.04 (0.23)	
$\Delta S$ in cal/mol.K	-0.64 (0.45)	

a) R. J. Abraham and R. H. Kemp, J. Chem. Soc. (B), 1971, 1240.

**A NON-INVASIVE METHOD TO DETECT THE DIFFERENCE IN FUNCTIONS OF  
CEREBRAL HEMISPHERES BY "DIFFERENTIAL NMR"**

Hirotake Kamei, Yoshiro Katayama, and Hiroshi Yokoyama  
Electrotechnical Laboratory, 1-1-4 Umezono, Sakura-mura  
Niihari-gun, Ibaraki 305

The functional difference of human cerebral hemispheres is one of the most important problems in the brain research. We describe here a novel (non-invasive) NMR technique to approach this subject. The method is based on the fact that the blood flow through the brain tissues varies inhomogeneously according to their levels of metabolism and functional activity, and that the inhomogeneous blood distribution is then to result in the variations of signals, in amplitude and in phase, gathered from region-selective NMR detectors located at several parts of the head surface. The present paper reports the results of a single differential detector consisting of two "surface coils." In spite of the crude nature of the experiment, however, we could clearly discern the enhanced blood supply to cortical areas that are activated by the performance of specific sensory, motor and mental tasks. We applied the technique to human volunteers and found that the left cerebral hemisphere played dominant roles in mathematical thinking and perception of musical rhythms, and the right hemisphere in the perception of melody. This is in accord with the current view of functional difference of hemispheres reached by means of PET(positron emission tomography), SPET(single photon emission tomography), etc.

## MOLECULAR DYNAMICS OF PYRIDINIUM IONS IN SOLID AS STUDIED

BY  $^1\text{H}$  NMRYukari Ito, Tetsuo Asaji, Ryuichi Ikeda, and Daiyu Nakamura

Department of Chemistry, Faculty of Science,

Nagoya University, Chikusa, Nagoya, Japan

Motions of pyridinium ions ( $\text{C}_5\text{NH}_6^+$ ) in crystals are expected to be analogous to those of benzene molecules in solid where random reorientational jumps of the molecule by  $60^\circ$  about its  $C_6$ -axis have been observed. The same motional mode of  $\text{C}_5\text{NH}_6^+$  ions, however, results in a dynamically disordered structure owing to the existence of the electric dipole moment of the ion. In fact, the presence of random orientations of the  $\text{C}_5\text{NH}_6^+$  dipoles between two opposite directions in the crystals was found in  $\text{C}_5\text{NH}_6[\text{AuCl}_4]$  by a study of X-ray diffraction at room temperature. According to this crystal structure, it is highly probable that the  $\text{C}_5\text{NH}_6^+$  reorientation takes place in a crystal field with a lower symmetry than  $C_6$ .

The temperature dependence of  $^1\text{H}$  NMR second moments ( $M_2$ ) in  $\text{C}_5\text{NH}_6[\text{AuCl}_4]$  showed a gradual  $M_2$  decrease from  $4.3 \text{ G}^2$  to  $0.9 \text{ G}^2$  with increasing temperature from 77 K to *ca.* 400 K. This  $M_2$  decrease can be explained well by the  $M_2$  calculation for the  $C_6$  reorientation model of the  $\text{C}_5\text{NH}_6^+$  ions about the pseudo- $C_6$  axes. However, the  $M_2$  decrease observed over a wide temperature range between *ca.* 120 and *ca.* 350 K cannot be attributed to a single motional process suggesting the existence of continuously distributed or several discrete correlation times of the reorientation.

The temperature dependence measurement of  $^1\text{H}$   $T_1$  of  $\text{C}_5\text{NH}_6[\text{AuCl}_4]$  at a Larmor frequency of 45.5 MHz yielded a  $\log T_1$  vs.  $T^{-1}$  curve with an asymmetric  $T_1$  minimum at 205 K which is unexplainable by the BPP theory. The observed  $T_1$  minimum value of *ca.* 590 ms was about five times longer than that predicted from the same theory. These experimental results were analyzed by assuming that the  $\text{C}_5\text{NH}_6^+$  ions reorient among three kinds of nonequivalent potential wells. Calculation based on this model gave an asymmetric  $T_1$  curve in good agreement with the observed one.



Observation of  $^{13}\text{C}$  Spin Exchanges in Solids  
by Two-Dimensional NMR Spectroscopy

Yi Yi Chen, Fumitaka Horii and Ryozo Kitamaru

Institute for Chemical Research, Kyoto Univ., Uji

$^{13}\text{C}$  spin exchanges in solids can be measured by combining CP/MAS  $^{13}\text{C}$  NMR spectroscopy with 2D NMR spectroscopy. Since the spin exchange rates must depend on the distances between spin pairs, it may be possible to obtain important information about the connectivity of carbon skeleton of an organic molecule by analyzing the spin exchanges. In this paper we have studied this possibility for some solid samples.

Solid-state 2D NMR spectra were measured at room temperature on JEOL JNM-FX200 spectrometer.  $^1\text{H}$  and  $^{13}\text{C}$  RF field strengths  $(\gamma B_1/2\pi)$  were 70 kHz. The MAS rate was 3.0-3.4 kHz. 2D data were analyzed using JEOL JNM-GX400 data system after transferred to the GX400 system and converted from FX format to GX format.

Figure 1 shows 2D  $^{13}\text{C}$  spin exchange spectrum of cellulose II crystals. Since the column points were so small as 128 (64 points were zero-filled) compared to 512 points for the  $F_2$  axis, data along the  $F_1$  and  $F_2$  axes are not symmetric. However, some cross peaks can be clearly observed.

Since three doublets at about 107, 89, and 64 ppm were unambiguously assigned to C1, C4 and C6 lines, respectively, other lines in the range of 72-79 ppm can be well assigned to C3, C5, and C2 carbons using the cross peaks between the respective doublets (Figure 1).

In contrast, it has been found that almost all carbon pairs have cross peaks in anhydrous  $\alpha$ -glucose crystals. This may be due to the strong dipolar interaction which favors  $^{13}\text{C}$  spin exchanges.

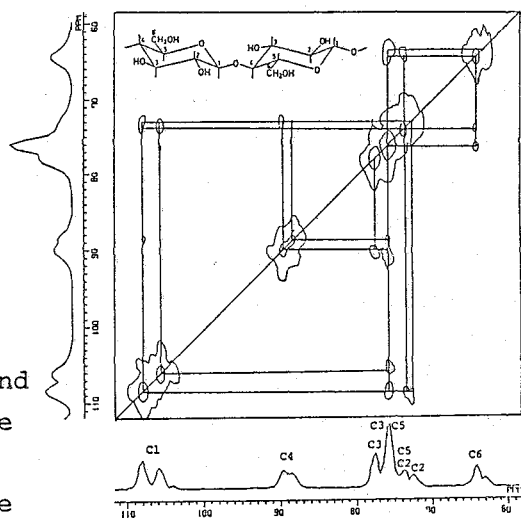


Fig.1 2D  $^{13}\text{C}$  spin exchange spectrum of cellulose II crystals. mixing time: 30s.

## CP/MAS $^{13}\text{C}$ NMR Study of $^1\text{H}$ Spin Diffusion

in the Polymeric Multi-Phase System.

Masaru Nakagawa, Fumitaka Horii and Ryozo Kitamaru

Institute for Chemical Research, Kyoto Univ., Uji

$^1\text{H}$  spin diffusion experiments are very useful in characterizing the spacial distribution of different phase-separated regions in polymer solids. In this paper, we have measured  $^1\text{H}$  spin diffusion process in polyethylene by combining Goldman-Shen pulse sequence with the  $^1\text{H}$ - $^{13}\text{C}$  cross-polarization procedure and analyzed the process by some structural models.

Bulk-crystallized liner polyethylene sample was used. CP/MAS  $^{13}\text{C}$  NMR spectra were measured at room temperature on JEOL JNM-FX200 NMR spectrometer.  $^1\text{H}$  and  $^{13}\text{C}$  RF field strengths  $\gamma B_1/2\pi$  were 69.4 kHz, while  $^1\text{H}$  dipolar decoupling field was reduced to 59.5 kHz. The contact time was 1 ms.

Figure 1 shows the result of  $^1\text{H}$  spin diffusion experiment. Here, we measured the spin diffusion process from the rubbery component to other components by observing the changes in  $^1\text{H}$  spins as those of  $^{13}\text{C}$  spins through the CP process. After each spectrum was resolved into the crystalline, interfacial, and rubbery components, the diffusion process was analyzed for each component using some structural models. As a result, it is found that the magnetization of the rubbery component first diffuse to the interfacial phase in the order of  $10^{-3}$  s. After averaged out in the noncrystalline region, the magnetization further diffuse to the crystalline phase in the order of  $10^{-2}$  s.

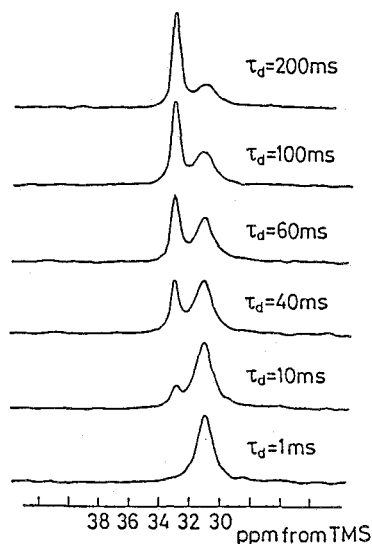


Fig.1  $^1\text{H}$  spin diffusion measurements

STRUCTURAL ANALYSIS OF PLASMA POLYMERIZED FILM BY  
HIGH-RESOLUTION SOLID-STATE NMR. POLYACRYLONITRILE.

Ichiro Tajima, Takako Suda, Minoru Yamamoto,  
Kozo Satta, and Hidetake Morimoto

Toyota Central Research and Development Laboratories, Inc.  
Nagakute-cho, Aichi, 480-11 Japan

Plasma treatment and plasma polymerization are known as effective methods for the surface modification, e.g. a control of the surface wettability. Plasma polymerization of acrylonitrile forms a hydrophilic thin film. The water contact angle of the surface is 50-65°. Plasma polymerization of that in nitrogen gas decreases the water contact angle to 40-50°. The surface wettabilities of plasma polymers are expected to depend on these chemical structures. High-resolution solid-state NMR technics were applied for structural analysis of the plasma polymerized acrylonitrile.

Plasma polymerization of acrylonitrile was carried out in the plasma reactor by the condition of pressure 13 Pa and power 100 W. NMR spectra of the polymers were measured by Fourier transform NMR spectrometer with superconducting magnet ( $^1\text{H}$  300 MHz at 7.0 Tesla). Observation nuclei;  $^{13}\text{C}$  and  $^{15}\text{N}$ . Methods; CP/MAS and CPDD/MAS (Cross Polarization with Delay Decoupling/Magic Angle Spinning).

Various types of amines (=N-) were formed from cyano group (-C≡N) in the plasma polymerization of acrylonitrile. In addition to the formation of carbon double bonds (-CH=CH-), carboxylic acids (-COOH) were also prepared in the air after the plasma polymerization. Plasma polymerization in the presence of nitrogen gas prepared the film included a large quantity of amine in the result of the stabilization of nitrogen radicals. In the region of electrode, cross-linked structures included heterocyclic structures by nitrogen and carbon atoms were found in the plasma polymerized film. These structural analyses revealed the plasma polymerization mechanism and that the surface wettability depended on the formation of amines and carboxylic acids in the plasma polymerization.

POLYMER STRUCTURE IN THE SOLID STATE AS STUDIED BY  $^{13}\text{C}$  VT-MAS NMR

Teruaki Fujito<sup>1</sup>, Kenzo Deguchi<sup>1</sup>, Mamoru Imanari<sup>1</sup>, Isao Ando<sup>2</sup>  
and Takeshi Yamanobe<sup>2</sup>

JEOL Ltd. Nakagami, Akishima-shi, Tokyo;<sup>2</sup>Department of Polymer  
Chemistry, Tokyo Institute of Technology, Ookayama, Meguro-ku,  
Tokyo

The  $^{13}\text{C}$  cross polarization/magic angle spinning (CP/MAS) NMR spectroscopy has proved to be a very powerful tool for structural analysis as a convenient probe of dynamic feature of polymers in the solid state. Usually,  $^{13}\text{C}$  CP/MAS NMR experiment has been carried out mainly at ambient temperature because of the difficulty for the variable-temperature(VT) spinner design. The experiment in conjunction with variable-temperature operation may present the potential for detailed insight into molecular structure and dynamics in the solid state.

The purpose of this work is to investigate the molecular structure of some polymers such as polyethylene and poly(L-glutamate) with n-alkyl side chain of long length as a function of temperature using  $^{13}\text{C}$  NMR(GX-270) spectroscopy equipped with VT-CP/MAS apparatus. From the  $^{13}\text{C}$  VT-CP/MAS experiments ( $-120^{\circ}\text{C}$  -  $120^{\circ}\text{C}$ ) for polyethylene, it was found that the fractions of the crystalline and amorphous states decrease and increase, respectively, as temperature is increased. On the other hand, from the  $^{13}\text{C}$  VT-CP/MAS experiments ( $25^{\circ}\text{C}$  -  $100^{\circ}\text{C}$ ) for poly(L-glutamate) with n-alkyl side chains, it was found that at room temperature the long alkyl side chains can be packed into n-paraffin-like crystallites and above  $35^{\circ}\text{C}$  they can attain the fast motion as a liquid paraffin, but the main chain takes the  $\alpha$ -helix form within the above temperature range.

$^{13}\text{C}$  NMR Chemical Shift and Electronic Structure of  
Cis and Trans Polyacetylenes in the Solid State

Takeshi Yamanobe and Isao Ando

Department of Polymer Chemistry, Tokyo Institute of Technology,  
Ookayama, Meguro-ku, Tokyo

A Recent development of the cross polarization-magic angle spinning (CP/MAS) NMR technique has provided useful information about the configuration of polyacetylenes in the solid state. It has been demonstrated that the  $^{13}\text{C}$  NMR signal of cis polyacetylene appears at about 10 ppm to low frequency of that of trans polyacetylene. In a previous report, we presented the formulae required to calculate the  $^{13}\text{C}$  NMR shielding and its tensor of polymers using the tight-binding (TB) MO theory based on the CNDO/2 method incorporated with the sum-over-state theory (SOS). It was shown that the calculation of the isotropic NMR chemical shift and the components of shielding tensor of polyacetylene, within the framework of CNDO/2 method, reproduces the experimental data qualitatively, but quantitative agreement was not satisfactory.

In this work, the calculation of  $^{13}\text{C}$  NMR chemical shift of polyacetylenes were carried out within the framework of INDO/S method which provides an understanding of photoelectron spectroscopy and gives more reliable excitation energies than the CNDO/2 method. It was found that the calculated  $^{13}\text{C}$  NMR chemical shift and its tensor agree with the experimental data fairly quantitatively.

The origin of difference between  $^{13}\text{C}$  NMR chemical shift calculated by INDO/S and CNDO/2 method was discussed with dividing calculated  $^{13}\text{C}$  NMR chemical shift into the contributions from each energy bands and with comparing charge density and bond orders.

HYDROGEN BONDING EFFECT ON THE  $^{13}\text{C}$  NMR CHEMICAL SHIFT OF GLYCINE RESIDUE CARBONYL CARBONS IN GLYCINE-CONTAINING PEPTIDES IN THE SOLID STATE

Shinji Ando<sup>1</sup>, Takeshi Yamanobe<sup>1</sup>, Isao Ando<sup>1</sup>, Akira Shoji<sup>2</sup>, Takuo Ozaki<sup>2</sup> and Shigetoshi Amiya<sup>3</sup>  
<sup>1</sup>Department of Polymer Chemistry, Tokyo Institute of Technology, Ookayama, Meguro-ku, Tokyo; <sup>2</sup>Department of Industrial Chemistry, College of Technology, Gunma University, Tenjin-cho, Kiryu-shi, Gunma; <sup>3</sup>Central Research Laboratory, Kuraray Co., Kurashiki-shi, Okayama

We have studied the relationship between the  $^{13}\text{C}$  chemical shift of polypeptides and its characteristic conformations, such as  $\alpha$ -helix,  $\beta$ -sheet,  $3_1$ -helix and  $\omega$ -helix forms, in the solid state. It was revealed that the  $^{13}\text{C}$  chemical shifts of individual amino acid residues in peptides are mainly depending on the local conformation of the residue under consideration.

For the carbonyl carbons in peptides, however, it was suggested that hydrogen bonding also takes an important role in determining its chemical shift by our study of collagen-like polypeptides and collagen fibrils, and by the another one of the conformational feature of  $^{13}\text{C}$  chemical shift tensors of glycine-residue carbonyl-carbons (Gly C=O) incorporated into some polypeptides which take various conformations.

For the purpose of elucidating the hydrogen bonding effect on the  $^{13}\text{C}$  chemical shift, we intended to observe the cross polarization/magic angle spinning (CP/MAS) spectra of the peptides which have a variety of hydrogen bond length in the polycrystalline state, of which the conformations were already determined by X-ray diffraction studies. A clear relationship was obtained for the hydrogen bond lengths and  $^{13}\text{C}$  chemical shift for the peptides. Therefore, We may explain reasonably the chemical shift displacements of Gly C=O in polyglycine and glycine-containing polypeptides by taking into account of the manner of hydrogen bonding.

$^{15}\text{N}$  CP-MAS NMR[III]. A STUDY ON THE RELATIONSHIP BETWEEN THE SOLID CONFORMATION AND THE  $^{15}\text{N}$  CHEMICAL SHIFT OF  $^{15}\text{N}$  LABELED L-ALANINE RESIDUES IN VARIOUS COPOLYPEPTIDES.

Akira Shoji<sup>1</sup>, Takuo Ozaki<sup>1</sup>, Teruaki Fujito<sup>2</sup>, Kenji Deguchi<sup>2</sup>,  
Shinji Ando<sup>3</sup>, Isao Ando<sup>3</sup>.

<sup>1</sup>Dept. Industrial Chemistry, College of Technology, Gunma University, Tenjin-cho, Kiryu, Gunma 376, Japan. <sup>2</sup>NMR Group, Analytical Instruments Technical and Engineering Division, JEOL Ltd., Nakagami, Akishima, Tokyo 196, Japan. <sup>3</sup>Dept. Polymer Chemistry, Tokyo Institute of Technology, Okayama, Meguro-ku, Tokyo 152, Japan.

We have previously found that  $^{15}\text{N}$  chemical shifts of homopolypeptides in the solid state depend on conformations such as  $\alpha$ -helix or  $\beta$ -sheet forms, amino acid residue and amino acid sequence.

In this study, we have synthesized various copolypeptides containing  $^{15}\text{N}$ -labeled L-alanine residue (about 5% and 20%), and investigated the relationship between the  $^{15}\text{N}$  chemical shift and the main chain conformation, amino acid residue, amino acid sequence by using the  $^{15}\text{N}$  cross polarization-magic angle spinning NMR. From these results, it was found that  $^{15}\text{N}$  chemical shift depends on conformation of solid copolypeptide, although  $^{15}\text{N}$  chemical shift value of L-alanine residue in copolypeptide is varied with the kind of amino acid residue in copolypeptide. This result is very interesting in comparison with the case of  $^{13}\text{C}$  chemical shifts which are not strongly influenced by a specific amino acid sequence. Further, we have measured powder pattern (static)  $^{15}\text{N}$  NMR spectra in order to obtain various kinds of  $^{15}\text{N}$  chemical shift tensors ( $\sigma_{11}$ ,  $\sigma_{22}$ ,  $\sigma_{33}$ ) of  $^{15}\text{N}$ -labeled amino acid residues of copolypeptides taking conformations such as  $\alpha$ -helix or  $\beta$ -sheet forms. These results showed that the  $^{15}\text{N}$  chemical shift tensors remarkably depend on conformation, amino acid residue and amino acid sequence. We conclude that the  $^{15}\text{N}$  NMR in the solid state is very useful to understand the polypeptide (or protein) structure.

CONFORMATION AND  $^{13}\text{C}$  NMR CHEMICAL SHIFT OF L-ALANINE RESIDUES  
INCORPORATED INTO POLY( $\beta$ -BENZYL L-ASPARTATE) IN THE SOLID STATE

Satoru Tuzi<sup>1</sup>, Tadashi Komoto<sup>1</sup>, Isao Ando<sup>1</sup>, Hazime Saito<sup>2</sup>,  
Akira Shoji<sup>3</sup> and Takao Ozaki<sup>3</sup>

<sup>1</sup>Department of Polymer Chemistry, Tokyo Institute of  
Technology, Ookayama, Meguro-ku, Tokyo; <sup>2</sup>Biophysics Division,  
National Cancer Center Research Institute, Tsukiji, Chuo-ku,  
Tokyo; <sup>3</sup>Department of Industrial Chemistry, College of  
Technology, Gunma University, Tenjin-cho, Kiryu-shi, Gunma

We have demonstrated by  $^{13}\text{C}$  NMR studies of polypeptides in the solid state, as measured by the CP/MAS technique, that  $^{13}\text{C}$  chemical shifts of the  $\text{C}_\alpha$ ,  $\text{C}_\beta$  and carbonyl carbons are considerably displaced, up to 7 ppm, depending on the particular conformations, such as  $\alpha$ -helix,  $\omega$ -helix and  $\beta$ -sheet forms. The existence of such conformation-dependent  $^{13}\text{C}$  chemical shifts and the collection of such data are very valuable in examining whether or not the conformation of polypeptide under consideration is retained in the solution state. This approach can be extended to probe local conformations of amino acid residues in peptides and proteins.

In this work, as a continuation of the above studies, we aim to obtain and discuss the relationship between the  $^{13}\text{C}$  chemical shift and conformation of poly( $\beta$ -benzyl L-aspartate) containing  $^{13}\text{C}$  enriched [ $3\text{-}^{13}\text{C}$ ]alanine residue as a minor component in the solid state, taking the antiparallel  $\beta$ -sheet, the right-handed  $\alpha$ -helix, the left-handed  $\alpha$ -helix and the left-handed  $\omega$ -helix forms by appropriate treatment. The latter two conformations for alanine residue are achieved only when alanine residues are incorporated in the poly( $\beta$ -benzyl L-aspartate), taking the respective conformations (Poly(L-alanine) takes only two conformations such as the right-handed  $\alpha$ -helix and antiparallel  $\beta$ -sheet forms in the solid state.). It is found that the alanine  $\text{C}_\beta$  chemical shifts are significantly displaced, depending on conformational change. These chemical shift data are expected to be used as reference data to examine conformation for alanine residues in proteins and also to examine whether or not conformation in the solid state is retained in the solution state.



DIRECT COMPARISON OF TERTIARY STRUCTURES BETWEEN THE SOLID  
AND SOLUTION STATE AS DETERMINED BY HIGH-RESOLUTION  $^{23}\text{Na}$   
NMR SPECTROSCOPY

Hazime Saitô and Ryoko Tabeta

Biophysics Div., National Cancer Center Research Inst.  
Tsukiji 5-chome, Chuo-ku, Tokyo, Japan

We have recently demonstrated that  $^{23}\text{Na}$  chemical shifts of sodium salts and complexes are significantly displaced (up to 60 ppm) depending on a variety of anions or ligand molecules and the Na-O interatomic distances, as determined by magic angle spinning.<sup>1</sup> Accordingly, it is now possible to examine whether or not conformations of sodium-complexed ionophores achieved in the solid state is retained in solution or membrane-bound state, by comparison of the  $^{23}\text{Na}$  chemical shifts in the solid and solution.

Here, we recorded  $^{23}\text{Na}$  NMR spectra of sodium complexes with naturally occurring and synthetic ionophores in chloroform solution.<sup>2</sup> The  $^{23}\text{Na}$  chemical shifts of sodium complexes with monensin and tetranactin obtained in chloroform solution are very close to those in the solid state, as a result of adopting similar conformation between the solid and solution. For the rest of complexes, however, the  $^{23}\text{Na}$  NMR signals are displaced downfield in solution as compared with those of the solid state: such downfield shifts are well interpreted in terms of the presence of conformational fluctuation and/or sodium ions interacting with solvent or anions. The presence of larger fluctuation-induced quadrupole coupling constants (up to 4.7 MHz) is consistent with our view about  $^{23}\text{Na}$  chemical shifts. These quadrupole interactions were reduced in methanol solution, owing to the presence of exchange with solvents.

1. R. Tabeta, M. Aida and H. Saitô, Bull. Chem. Soc. Jpn., 59, 1957 (1986).
2. H. Saitô and R. Tabeta, Bull. Chem. Soc. Jpn., in press.

CONFORMATIONAL CHANGE OF IONOPHORE ANTIBIOTICS BY METAL-ION  
BINDING AS DETECTED BY HIGH-RESOLUTION SOLID-STATE  $^{13}\text{C}$  NMR

Hazime Saitô and Ryoko Tabeta

Biophysics Div., National Cancer Center Research Inst.

Tsukiji 5-chome, Chuo-ku, Tokyo, Japan

We previously showed that sizable conformation-dependent  $^{13}\text{C}$  chemical shifts (up to 8 ppm) are accompanied by a conformational change of a variety of ionophores complexed with metal ions.<sup>1,2</sup> In addition, the existence of such conformation-dependent displacements of  $^{13}\text{C}$  chemical shifts have been so far demonstrated for a variety of molecular systems such as peptides, polypeptides, polysaccharides, etc.<sup>3,4</sup>

Here, we further examined high-resolution solid-state  $^{13}\text{C}$  NMR spectra of nonactin and tetranactin complexed with mono- and divalent cations such as  $\text{NH}_4^+$ ,  $\text{Rb}^+$ ,  $\text{Ca}^{2+}$ , and  $\text{Ba}^{2+}$ . We found that the carbonyl (C-1)  $^{13}\text{C}$  chemical shifts of nonactin and tetranactin are displaced substantially downfield at about 180-183 ppm, as compared with those of the complexes with alkali cation (178 ppm). Obviously, such a significant change in the  $^{13}\text{C}$  chemical shifts could be ascribed to the presence of distorted conformation of ligand molecules. In fact, further displacements of peaks other than the C-1 carbons are noted for these complexes. In addition, we showed that the C-1  $^{13}\text{C}$  chemical shifts are well related to the torsion angles O'1-C1-C2-C3 as determined by X-ray diffraction, for the complexes whose X-ray diffraction data are available. Finally, we compared the  $^{13}\text{C}$  chemical shifts of these complexes between the solid and solution, to gain a clue how the solid-state conformation could be retained in solution.

1. R. Tabeta and H. Saitô, *Biochemistry*, 24, 7696 (1985)
2. R. Tabeta and H. Saitô, *Bull. Chem. Soc. Jpn.*, 58, 3215 (1985).
3. H. Saitô, *Magn. Reson. Chem.* in press.
4. H. Saitô, et. al. in "Magnetic Resonance in Biology and Medicine", Tata McGraw-Hill, p.195, 1985.





